Role of CXCL5–CXCR2 axis in oral squamous cell carcinoma invasion

Hyungkeun Kim

Department of Applied Life Science

The Graduate School, Yonsei University

Role of CXCL5–CXCR2 axis in oral squamous cell carcinoma invasion

The Doctoral Dissertation Submitted to
the Department of Applied Life Science,
the Graduated School of Yonsei University
in partial fulfillment of the requirements
for the degree of Doctor of Philosophy

Supervised by Dr. Won-Yoon Chung

Hyungkeun Kim

June 2021

This certifies that the Doctoral Dissertation of Hyungkeun Kim is approved.

Thesis supervisor: Won-Yoon Chung

Jeong-Heon Cha

Na-Young Song

Dong wook Kim

Xianglan Zhang

The Graduate School

Yonsei University

June 2021

ACKNOWLEDGEMENTS

I would like to thank all of those with whom I have had the pleasure to my work during my PhD degree course. First of all, I am grateful to the committee members, Prof. Won-Yoon Chung, Prof. Jeong-Heon Cha, Prof. Na-Young Song, Prof. Dong Wook Kim, and Prof. Xianglan Zhang for their advice and feedback. Their profound perspectives have helped me to strengthen my work. Especially, I would like to express my deepest gratitude to my supervisor Prof. Won-Yoon Chung for her enduring support and practical advice, which has urged me to complete my study. As my teacher and mentor, she has taught me what a good scientist should be.

I hope to give my thanks to all professors and colleagues of the Department of Oral Biology for experimental and moral support. Also, I would like to thank my friends and co-workers in my biochemistry laboratory for their warm encouragement and positive energy during my dissertation.

Finally, I would like to acknowledge with the deep appreciation to my family, my parents, grandparents, and my younger sister's family for constant dedication and care. Especially, I would like to express my special gratitude to my honorable love for her passionate affection, advocates, and patience.

Hyungkeun Kim

TABLE OF CONTENTS

LIST OF FIGURES

LIST OF TABLES

ABSTRACT

Role of CXCL5-CXCR2 axis in oral squamous cell carcinoma invasion

Hyungkeun Kim

Department of Applied Life Science

The Graduate School, Yonsei University

(Directed by Professor Won-Yoon Chung)

Oral squamous cell carcinoma (OSCC) is the most common malignant neoplasms of the oral cavity. Anatomically, advanced oral cancer readily invades and destroys the maxilla and mandibular bones. OSCC-induced invasion is correlated with poor prognosis and still relatively unfavorable. In this study, I aimed to determine the role of CXCL5 and CXCR2 in OSCC cell invasion and their underlying molecular mechanisms.

Treatment with CXCL5 promoted cell invasion but treatment with neutralizing antibody against CXCL5 inhibited cell invasion in OSCC cells. Neutralization of

CXCR2 with its specific antibody or shRNA-transfected CXCR2 knockdown markedly blocked OSCC cell invasion in the absence or presence of CXCL5. CXCR2 knockdown transformed cell morphology into cobblestone-like phenotype which is correlated with weak invasiveness.

Gene set enrichment analysis using RNA-seq data showed interferon alpha response- and reactive oxygen species pathway-related genes were enriched in CXCL5-treated OSCC cells. In addition, CXCL5 treatment upregulated the transcriptional activity of NF-κB, HIF-1α, and AP-1 and CXCL5/CXCR2 signaling increased the expression levels of NF-κB and IκBα and phosphorylation of NF-κB and AKT. Treatment with NF-κB or AKT inhibitors significantly blocked OSCC cell invasion in the absence or presence of CXCL5. Treatment with NF-κB inhibitor blocked CXCL5-induced expression levels of NF-κB and but did not inhibit CXCL5-induced phosphorylation of AKT. Treatment with AKT inhibitor blocked CXCL5-induced expression of NF-κB and IκBα and AKT phosphorylation.

In bioinformatics analysis, *CXCL5* is associated with more advanced stage and poor prognosis of oral cancer and positively correlated with *NFKB1* and *IKBA* expression.

In conclusion, CXCL5 promotes OSCC cell invasion by activating AKT/NF-κB via CXCR2. CXCL5, CXCR2, and their downstream molecules are helpful biomarkers for the prediction of OSCC invasion.

Keywords: oral cancer, OSCC, invasion, CXCL5, CXCR2, NF-κB, AKT

Role of CXCL5-CXCR2 axis in oral squamous cell carcinoma invasion

Hyungkeun Kim

Department of Applied Life Science

The Graduate School, Yonsei University

(Directed by Professor Won-Yoon Chung)

Ⅰ. Introduction

Oral cancer belongs to head and neck cancers and is considered to be one of the most commonly occurring cancers through the world[1,2]. Oral squamous cell carcinoma (OSCC) constitutes 90% of all head and neck cancers[3]. Owing to late detection or diagnosis at advanced stages, five-year survival rate of oral cancer patients has not improved substantially in the past 20 years and is poor at 66% for all races[2, 4]. The recent World Health Organization classification of head and neck tumors indicated that conventional histological grading (well, moderate, or poorly differentiated OSCC) and pattern of cell invasion (non-cohesive pattern of invasion, perineural and

lymphovascular invasion, and bone invasion) in OSCC are associated with poorer prognosis[5]. Especially, OSCC is anatomically related to jaw and frequently invades the maxillary or mandibular bone[6]. The American Joint Committee on Cancer (AJCC) staging system offers TNM (tumor, node, and metastasis) classification and oral cancer invasion through bone of mandible or maxilla was classified as T4a[7,8]. With reflection of progressively advanced extent of disease, the bone destruction induced by carcinoma invasion lowers cancer patients' survival and quality of life (QOL)[8, 9]. Therefore, more precise prediction markers for OSCC invasion are required for early detection and appropriate treatment.

Bone is a mineralized connective tissue and exerts diverse function, such as protecting against external damage, structural support for organs, and storage and provision of minerals. For maintaining bone homeostasis, osteoblasts, osteoclasts, osteocytes, and stromal cells interact with each other through cytokines and growth factors[10, 11]. However, once OSCC invades the mandibular bone, bone homeostasis becomes imbalanced and bone resorption is predominantly induced[12]. OSCC cell-secreted cytokines, including monocyte chemoattractant proteins-1[13], parathyroid hormone-related peptide[14], interleukin-6[15], and receptor activator of nuclear factor κB ligand (RANKL)[16, 17] induce differentiation and activation of osteoclasts from osteoclast precursor cells, causing osteolysis. To establish diagnostic and therapeutic strategies for OSCC bone invasion, novel molecular biomarkers detectable in saliva, serum, and tumor tissues should be determined.

C-X-C motif chemokine 5 (CXCL5), also known as epithelial cell-derived neutrophil-activating peptide-78 (ENA-78), is upregulated in more than 14 different malignant tumor types, including breast[18, 19], prostate[20, 21], and lung cancer[22] and increases the proliferation, migration, and invasion of these cancer cells[23]. In the case of breast cancer cells, CXCL5 promotes cell migration and invasion through extracellular signal-regulated kinase (ERK), mitogen- and stress-activated protein kinase 1 (MSK-1), and ETS domain-containing protein Elk-1 (Fig. 1A)[18]. Furthermore, the secretion of CXCL5 is increased in breast cancer-associated bone marrow cells and osteoblasts and the secreted CXCL5 facilitates the extravasation into bone and colonization in bone of breast cancer cells[19]. In prostate tumor microenvironment, CXCL5 is secreted from macrophage-driven efferocytosis of prostate cancer cells via signal transducer and activator of transcription 3 (STAT3) and nuclear factor kappa B (NF-κB) signaling[20]. Enhanced secretion level of CXCL5, in malignant prostatic tissues, acts as a crucial chemoattractant of inflammatory myeloid cells and induces M2 polarization which results in perpetual inflammation and immunosuppression[21]. CXCL5 is secreted from macrophages in the gastric cancer microenvironment and promotes gastric cancer cell migration via STAT3 signaling pathway (Fig. 1B)[24]. CXCL5–CXC chemokine receptor 2 (CXCR2) axis contributes to cell migration and invasion by enhancing epithelial to mesenchymal transition (EMT) through protein kinase B (AKT), glycogen synthase kinase-3 (GSK-3), and β-catenin pathway in lung cancer cells[25] and nasopharyngeal carcinoma cells (Fig. 1C)[26]. In addition, CXCL5

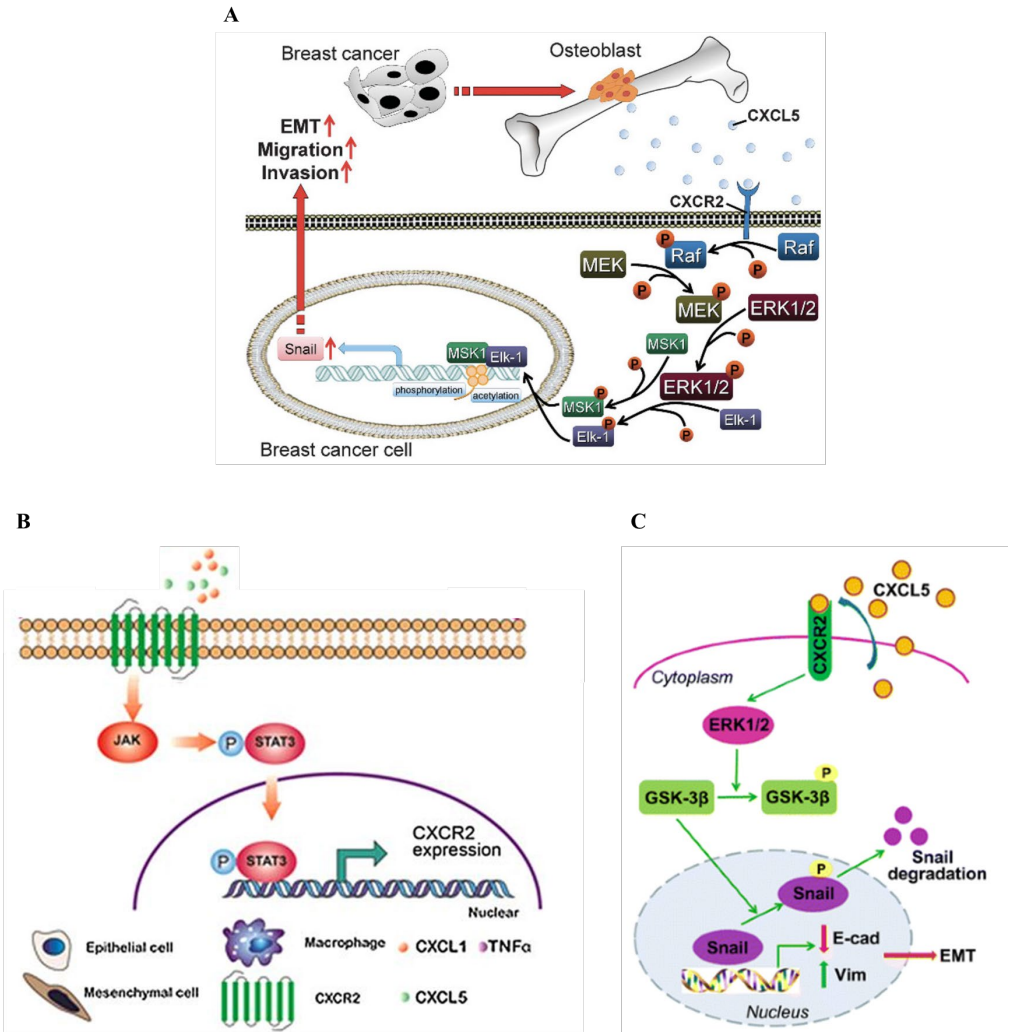

Figure 1. Schematic representation of CXCL5 signaling pathway in various cancer cell types. CXCL5 signaling pathway in (A) breast cancer cells[18], (B) gastric cancer cells[24], and (C) nasopharyngeal carcinoma cells[26].

also recruits lots of cancer-associated inflammatory cells, cancer-associated fibroblasts[21], and tumor-associated neutrophils into tumor microenvironment[27] and forms a feed forward loop with increased cancer metastasis[28]. In diverse cancer types, CXCL5 has negative correlation with cancer patients' QOL[19] and survival[23]. Furthermore, CXCL5 is expressed by many immune cells and mediates inflammation related-diseases, such as arthritis[29], neuroinflammation[30], and chronic obstructive pulmonary disease[31]. In bone, CXCL5 has been reported to increase RANKL expression and secretion through ERK and p38 MAPKs in osteoblasts[32]. However, the role of CXCL5 in oral cancer invasion remains unclear.

CXCR2 is a member of G protein coupled receptor (GPCR) family and binds to various CXC chemokines, including CXCL1, CXCL2, CXCL3, CXCL5, CXCL6, CXCL7, and CXCL8. These chemokines with Glu-Leu-Arg (ELR) motif have been firstly known as neutrophil chemotactic factors and potent promoters of angiogenesis. According to analysis of immune and cancer cells, binding of CXCLs to CXCR2 has cellular events, including inflammation and cancer migration, invasion, and proliferation, by activating phosphoinositide 3-kinase (PI3K), p38/ERK, and Janus kinase (JAK) pathways (Fig. 2)[23]. In addition, CXCR2 silencing reduces the migration and invasion of OSCCs[33]. CXCL8, secreted by OSCC, binds to exclusively CXCR2 in bone marrow stem cells (BMSCs) and facilitates recruitment of BMSCs to OSCC. Tumor growth factor-β (TGF-β) secreted from BMSCs induces EMT and promotes the proliferation, migration, and invasion in OSCC cells[34]. OSCC-derived CXCL1

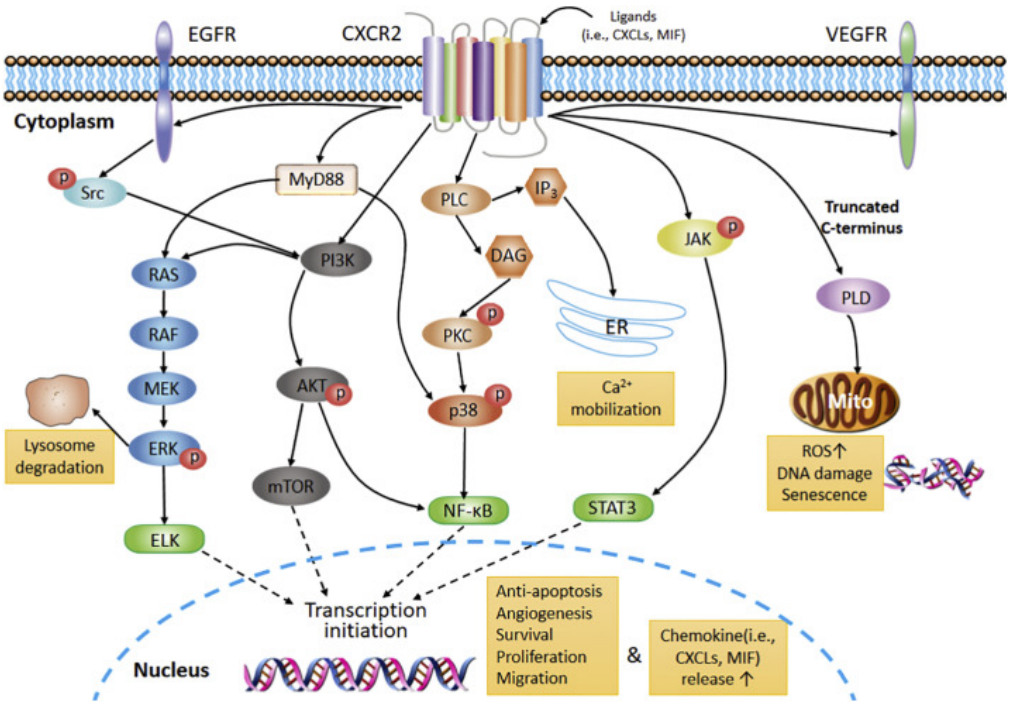

Figure 2. Schematic representation of CXCLs/CXCR2 signaling pathway[23].

induces transition of normal fibroblasts into cancer-associated fibroblasts[35]. CXCL1[36], CXCL2[37], and CXCL8[38] act as chemoattractant factors for osteoclast precursors and induce differentiation and activation of osteoclasts. However, CXCL5-CXCR2 signaling in OSCC has not yet identified.

In this study, I attempted to determine the role of CXCL5-CXCR2 axis in OSCC invasion and its downstream target molecules with potential as promising biomarkers for OSCC invasion.

Ⅱ. Materials and Methods

1. Reagents and antibodies

Dulbecco's modified Eagle's medium (DMEM), Roswell Park Memorial Institute (RPMI) 1640, fetal bovine serum (FBS), Hank's balanced salt solution (HBSS), phosphate-buffered saline (PBS), antibiotic-antimycotic mixture containing 100 U/ml penicillin, 100 μg/ml streptomycin, and 0.25% trypsin-ethylenediaminetetraacetic acid (EDTA) were purchased from Gibco BRL (Grand Island, NY, USA). Recombinant human CXCL5 was obtained from R&D system (Minneapolis, MN, USA). Propidium iodide (PI), 3-(4,5-dimethylthiazol-2yl)-2,5-diphenyl tetrazolium bromide (MTT), gelatin from porcine skin, bovine serum albumin (BSA), dimethyl sulfoxide (DMSO), and puromycin were purchased from Sigma-Aldrich Chemical (St. Louis, MO, USA). 2',7'–dichlorofluorescin diacetate (DCFDA) was purchased from Thermo Fisher Scientific (Waltham, MA, USA). Matrigel was purchased from BD Biosciences (Palo Alto, CA, USA). The selective inhibitor of AKT1/2/3, MK-2206 2HCL and the selective inhibitor of NF-κB, JSH-23 were purchased from Selleckchem (Houston, USA). All reagents used in this study were of analytical grade.

The antibodies were obtained from the following sources: polyclonal anti-rabbit antibodies against p65, phosphorylated inhibitor kappa B alpha at serine 32/36 (p-IκBα), Lamin B1, and AKT and monoclonal anti-mouse antibodies against CXCL5, CXCR2, glyceraldehyde 3-phosphate dehydrogenase (GAPDH), phosphorylated p65

at serine 311 (p-p65), IκBα, and phosphorylated AKT at serine 473 (p-AKT); anti-CXCL5 (MAB254) and anti-CXCR2 (MAB331) antibodies (R&D system); anti-p-p65 (sc-166748) and anti-IκBα (sc-371) antibodies (Santa Cruz Biotechnology, Santa Cruz, CA, USA); anti-p-p65 NF-κB (#3034), anti-p-IκBα (#9246), anti-AKT (#4691), and anti-p-AKT (#9276) antibodies and horseradish peroxidase (HRP) conjugated anti-mouse (#7076) and rabbit (#7074) secondary antibodies (Cell Signaling Technology, Danvers, MA, USA); anti-rabbit β-actin polyclonal antibody (Sigma-Aldrich); and allophycocyanin (APC) crosslinked goat anti-mouse IgG (Invitrogen).

2. Cell culture

Ca9-22, HSC-2, and HSC-3 OSCC cells were purchased from Japanese Collection of Research Bioresources Cell Bank (Shinjuku, Japan). YD-10B OSCC cells were obtained from the Department of Oral pathology, Yonsei University College of Dentistry (Seoul, Korea). Ca9-22 and HSC-2 OSCC cells were derived from gingiva and floor of cavity, respectively, and the primary site of YD10-B and HSC-3 OSCC cells is tongue. The cells were grown in DMEM supplemented with 10% FBS and 1% antibiotic-antimycotic mixture at 37˚C in a humidified 5% CO_2.

3. Cell viability assay

OSCC cells (1×10^3 cells/well) were seeded in 96-well plates and treated with CXCL5 at the indicated concentrations for 24 h or 72 h. CXCR2 shRNA-transfected

cells (1×10^3 cells/well) were incubated for 24 h. The cells were incubated with 20 μl MTT (5 mg/ml) in PBS at 37˚C for 4 h. The medium was removed, and the cells were lysed with 200 μl DMSO for 30 min at 37˚C. Absorbance was determined at 570 nm using a microplate reader (Bio-Rad Laboratories, Hercules, CA, USA).

4. Transwell invasion assay

The invasive ability of OSCC cells was determined using a 6.5 mm transwell chamber with an 8.0 μm pore polycarbonate membrane (Corning Costar, Lowell, MA, USA). The lower and upper surfaces of the membrane were coated with 10 μl gelatin (1 mg/ml in distilled water) and 40 μl Matrigel (1 mg/ml in distilled water), respectively. OSCC cells (5×10^4 cells/0.2 ml) were seeded in the upper chamber with the complete medium containing 0.5% FBS and indicated concentrations of CXCL5, anti-CXCL5, or anti-CXCR2 in the absence or presence of MK-2206 2HCL or JSH-23. The lower chamber was filled with 0.6 ml of the complete medium containing 10% FBS and the indicated concentration of CXCL5, anti-CXCL5, or anti-CXCR2 in the absence or presence of MK-2206 2HCL or JSH-23. After a 24 h incubation, the cells were fixed with 70% methanol and the membranes were stained with Mayer's hematoxylin (Cancer diagnostics, Durham, NC, USA). Non-invaded cells on the upper surface of the membrane were gently removed with cotton swabs. The number of the invaded cells was then imaged and counted using imageJ software (NIH, v1.48)[39]. The representative images at x40 magnification were acquired using Leica DMi1 inverted

Microscope (Leica, Wetzlar, Germany).

5. Reverse Transcription-Polymerase Chain Reaction (RT-PCR)

Total RNA was extracted using Ambion® TRIzol reagent (Thermo Fisher Scientific) and the quality of RNA was checked using µDrop™ Plate (Thermo Fisher Scientific). cDNA was synthesized using 1 µg of total RNA and CellScript™ All-in-One 5X First Strand cDNA Synthesis Master Mix (CellSafe, Yongin, Korea) in accordance with the manufacturer's instructions. cDNA was amplified using Tetro cDNA synthesis Kit (Taunron, MA, USA) and the PCR products were analyzed on 1.5% agarose gel. The following primers were used: *CXCR2* forward: 5'- CTTTTCTACTAGATGCCGC-3', reverse: 5'- AGATGCTGAGACATATGAATTT-3'; *GAPDH* forward: 5' – ACCACAGTCCATGCCATCAC-3', reverse: 5'- TCCACCACCCTGTTGCTGTA-3'

6. RNAi-mediated gene silencing

To establish OSCC cells with stable knockdown of CXCR2 (Locus ID: 3579), the cells were transduced with shRNA lentiviral particles (ORIGENE, Rockville, MD, USA). One negative control shRNA (TR30021V) and four different CXCR2 shRNAs (TL312157VA: shRNA-1, TL312157VB: shRNA-2, TL312157VC: shRNA-3, and TL312157VD: shRNA-4) were used. OSCC cells were seeded in 60-mm dishes and the cells were incubated with viral supernatants in the presence of 10 µg/ml polybrene (Santa Cruz Biotechnology) for 24 h. After the viral supernatants were removed, the

infected cells were cultured in fresh medium containing 10% FBS for 2 days and then incubated in medium containing 10% FBS and 5 μg/ml puromycin for an additional 2 weeks. For quantification of the expression level of CXCR2, the cells (1 x 10^6 cells) were incubated in 100 mm dish for 24 h and then harvested with trypsin EDTA. The cells were washed with PBS, centrifuged at 500 x g for 3 min, and then fixed with 2% paraformaldehyde in PBS for 30 min in room temperature. After fixation, the cells were permeabilized with 0.1% Triton® X-100 buffer (Amresco Inc., Solon, OH, USA) for 20 min at room temperature and then blocked with 0.5% BSA and 2% FBS in PBS buffer. The cells were stained with anti-CXCR2 (1:2,000) and APC crosslinked-secondary antibody (1:5,000). The level of CXCR2 in OSCC cells was quantified by using BD FACS verse II (BD Biocsiences, San Jose, USA).

7. RNA sequencing (RNA-seq) and data analysis

Ca9-22 cells were treated with vehicle or 50 ng/ml CXCL5 for 6 h or 24 h. Total RNA of Ca9-22 cells was extracted with TRIzol reagent. DNA contamination was removed with DNase (Thermo Fisher Scientific) and the quality of RNA was checked using μDrop™ Plate. The extracted RNA samples were used for library preparation. The preparation of whole transcriptome libraries and sequencing were conducted by Macrogen Inc. (Seoul, Korea). The sequencing library was prepared by random fragmentation of the cDNA sample, followed by 5’ and 3’ adapter ligation. Adapter-ligated fragments were then amplified by PCR. For cluster generation, the library was

loaded into a flow cell where fragments were captured on a lawn of surface-bound oligos complementary to the library adapters. Each fragment was then amplified into distinct and clonal clusters through bridge amplification. After cluster generation, the samples were sequenced in an Illumina NovaSeq 6000 System sequencer. The quality of paired end reads of all 16 samples was checked by FASTQC (v0.11.7) program. Low quality bases and adapter sequences were removed with Trimmomatic software (version 0.36). Only good quality trimmed reads were considered for downstream analysis. Alignment with HISAT2, the reads in the FASTQ files were mapped to a reference genome. After read mapping, transcript assembly was executed using StiringTie program and expression values in Transcripts Per Kilobase Million (TPM) and Fragments Per Kilobase Million (FPKM) values were generated along with read coverage stats for the transcript and individual exons. From FPKM values, gene-set enrichment analysis (GSEA, http://www.broadinstitute.org/gsea/index.jsp), a method to determine that if predefined sets of genes are differentially expressed in different phenotypes[40], was performed to detect any possible signal pathway sets of genes showing statistically significant differences by treatment of CXCL5.

8. Pathway reporter array

To investigate the transcriptional activities regulated by CXCL5 and CXCR2 in OSCC cells, the Cignal Finder 45-Pathway Reporter Array (SA Biosciences) was conducted according to the manufacturer's instructions. The array contains

expression plasmids that harbor specific promoters, indicating changes in 45 transcription factor activities together with control and normalizing plasmids. Ca9-22 cells and CXCR2 knockdown cells were reversely transfected onto a 96 well, which contains the reporter plasmids spotted, for 24 h, and the transfected cells were treated with vehicle or 50 ng/ml CXCL5 for 24 h. Luciferase activity was measured using the Dual Luciferase Assay system (Promega, Madison, WI, USA) with a luminescence microplate reader (Varioskan Flash 3001, Thermo Fisher Scientific). *Firefly* luciferase activities were normalized over *Renilla* luciferase activities after subtraction of background activity determined by luciferase activities of negative controls. The fold change in each transcriptional activity was calculated from the normalized luciferase activities in treated versus untreated cells.

9. Measurement of intracellular reactive oxygen species (ROS)

OSCC cells (5 x 10^5 cells) were seeded in 60 mm culture dish and treated with CXCL5 at indicated concentration in serum-free DMEM for 24 h. The cells were trypsinized and centrifuged at 500 x g for 3 min. The harvested cells were incubated with 20 μM DCFDA dye (diluted in 1 ml of distilled water) for 30 min at 37˚C. After the supernatants containing DCFDA were removed, the stained cells were resuspended in 100 μl of PBS and analyzed with flow cytometry using 485 nm laser for excitation and 535 nm for emission.

10. Western blot analysis

OSCC cells (1 x 10^6 cells) were seeded in 100 mm culture dish and treated with CXCL5 at indicated concentration in serum-free DMEM for 24 h. Cell lysates were prepared using radioimmunoprecipitation assay (RIPA) buffer containing a protease inhibitor cocktail (Cell Signaling Technology) and 1 mM phenylmethylsulfonyl fluoride (Sigma-Aldrich). The lysates were centrifuged at 20,000 x g for 20 min at 4˚C. Nuclear and cytosolic fractions were obtained from OSSC cell lysates using a nuclear/cytosol fractionation kit (BioVision, Mountain View, CA, USA) according to the manufacturer's instructions. The protein concentration was determined using a bicinchoninic acid (BCA) kit (Pierce, Rockford, IL, USA). Protein (40 μg) was loaded onto a sodium dodecyl sulfate-polyacrylamide gel and electrophoresed. The proteins were then transferred to a polyvinylidene difluoride membrane (Millipore, Danvers, MA, USA). The membrane was blocked with 10% skim milk in Tris-buffered saline (10 mM Tris, pH 8.0, and 150 mM NaCl) with 0.1% Tween-20 (TBS-T) and then incubated with primary antibodies (1:1,000) in TBS-T containing 3% BSA. The membrane was further incubated with HRP-conjugated secondary antibodies in TBS-T containing 3% skim milk for 1 h at room temperature. The targeted proteins were visualized with Amersham ECL Western Blotting Detection Reagents (GE healthcare, Little Chalfont, UK) and detected using Amersham imager 600.

11. Public database analysis

CXCL5 and *CXCR2* mRNA expressions in various cancer patients were analyzed using ONCOMINE database. The cut-off of P value, fold change, and gene rank were defined as 0.01, 2, and top 10%, respectively. Head and neck cancer datasets were generated by The Cancer Genome Atlas (TCGA) Research Network (http://cancergenome.nih.gov/). TCGA Head and neck cancer data were obtained from The Human Protein Atlas (http://www.proteinatlas.org) in February 2021 to analyze *CXCL5* and *CXCR2* gene expression levels in head and neck cancer tissues (n = 499). The data retrieved from the TCGA website were reanalyzed to determine Pearson's correlation coefficients (r) between *CXCL5* mRNA and target mRNAs (*RELA, NFKB1,* and *IKBA*) and the correlation of overall survival, stage, and expression levels of related genes.

12. Statistics

Statistical analyses were performed using Statistical Package for Social Sciences (SPSS) version 19.0 software (SPSS Inc., New York, NY, USA). The results are expressed as the mean ± SEM. Data were analyzed by 2-tailed unpaired Student's t test for comparisons between 2 groups and one-way Analysis of variance (ANOVA) with relevant post hoc tests for multiple comparisons. A P value less than 0.05 was considered statistically significant. In public database analysis, the data retrieved from TCGA website were reanalyzed using GraphPad Prism 7 and SPSS (GraphPad

Software, San Diego, CA, USA). Pair-wise Pearson's correlation coefficient value was used to determine the relation between *CXCL5* mRNA and target mRNAs. Kaplan-Meier survival curves were compared using the log-rank test.

Ⅲ. Results

1. CXCL5 increased the viability and invasion of several OSCC cells

Malignant tumor progression is related with high proliferative and invasive ability of cancer cells[41]. CXCL5 treatment for 24 h and 72 h significantly increased the viability of Ca9-22 and YD-10B cells, but did not affect that of HSC-2 and HSC-3 cells (Fig. 3). In transwell invasion assay, treatment with 50 ng/ml CXCL5 accelerated the invasion of Ca9-22, YD-10B, and HSC-3 cells by 3.48, 5.87, and 17.11-fold, respectively (Fig. 4A). CXCL5 neutralization by 20 μg/ml anti-CXCL5 diminished the invasion of YD-10B and HSC-3 cells invasion by 30% and 25%, respectively (Fib. 4B). Ca9-22 cell invasion was inhibited by 18% by treatment with 40 μg/ml anti-CXCL5, However, that of HSC-2 cells was not affected by treatment with CXCL5 or anti-CXCL5. These results indicate that CXCL5 can promote invasion in OSCC cells in paracrine and autocrine manners.

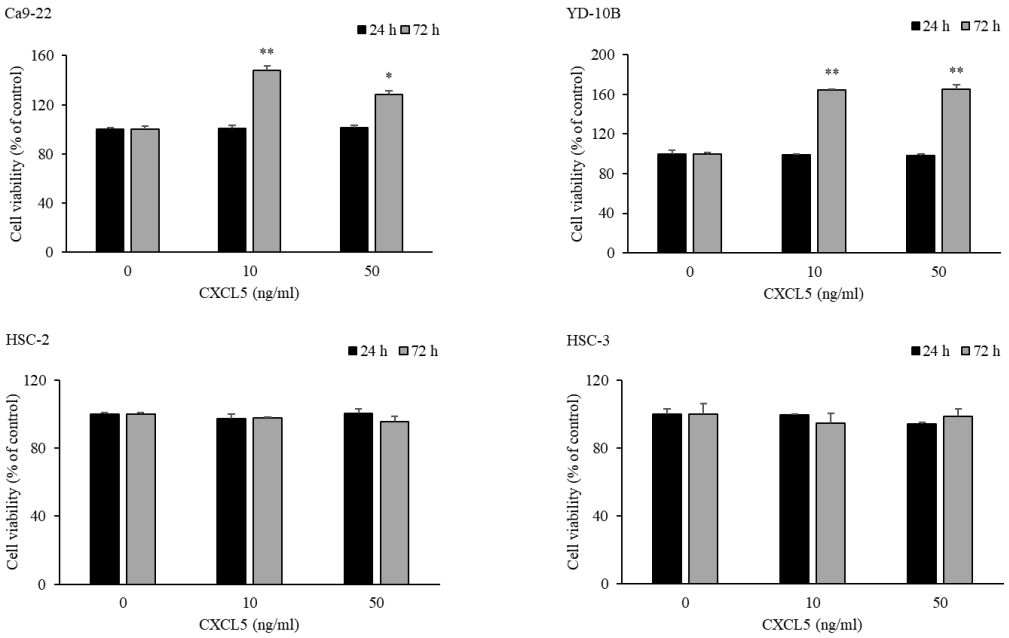

Figure 3. CXCL5 increased several OSCC cell viability. Ca9-22, YD-10B, HSC-2, and HSC-3 cells ($1x10^3$ cells/well) were treated with 10 and 50 ng/ml CXCL5 for 24 h and 72 h, respectively. Cell viability was determined using an MTT assay. * $P < 0.01$, ** $P < 0.001$ versus untreated cells.

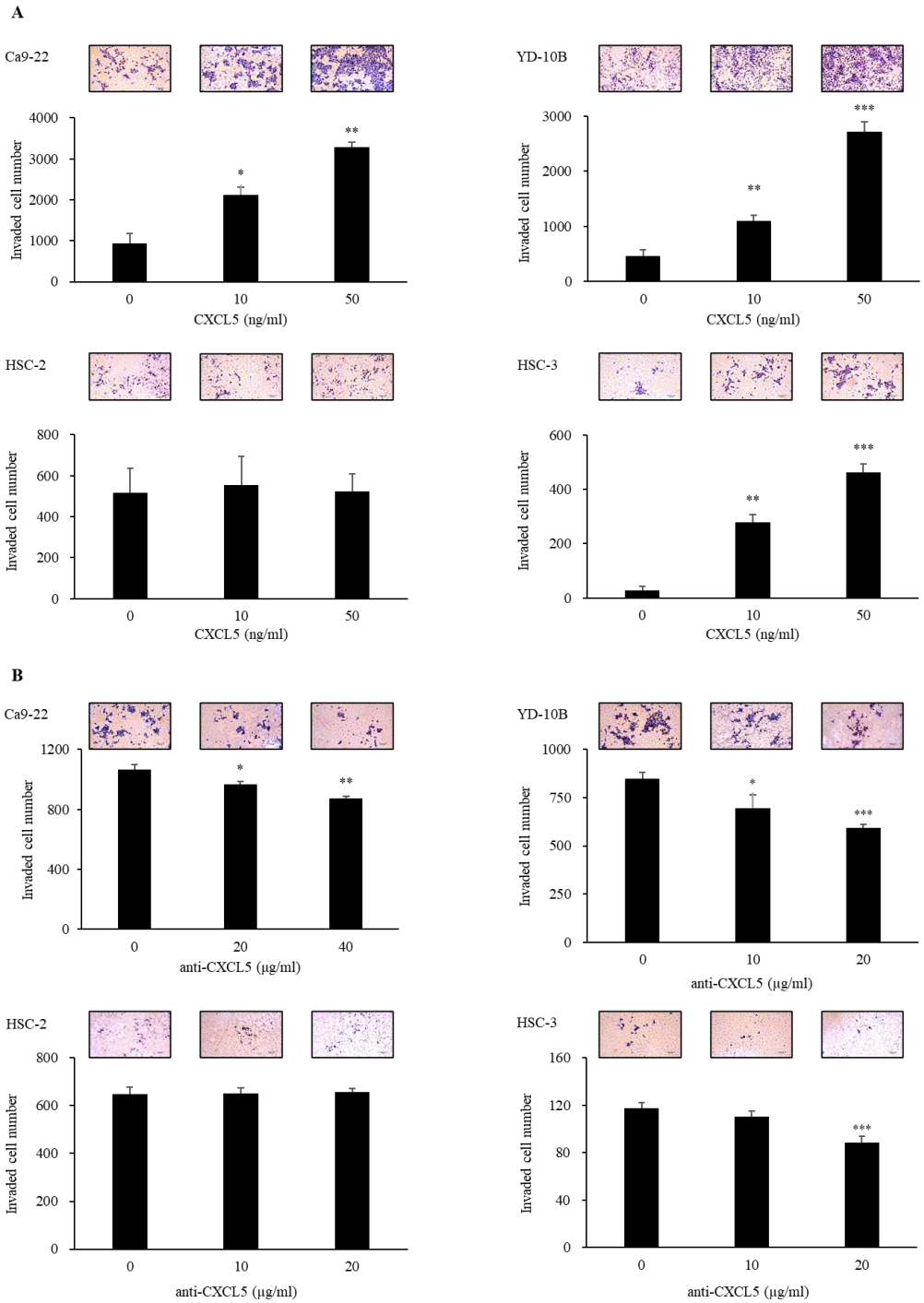

Figure 4. CXCL5 increased several OSCC cells invasion. (A, B) Ca9-22, YD-10B, HSC-2, and HSC-3 cells ($5x10^4$ cells/well) were seeded into Matrigel-coated upper chamber. DMEM containing 0.5% FBS and 10% FBS in the presence of (A) CXCL5 or (B) anti-CXCL5 at the indicated concentrations were added into upper and lower chamber, respectively. The cells were incubated for 24 h. The invaded cells were fixed, stained with hematoxylin, and counted using Zeiss Axio imager microscope (original magnification, 40x). * $P < 0.05$, ** $P < 0.01$, *** $P < 0.001$ versus untreated cells.

2. CXCL5 increased Ca9-22 and YD-10B cell invasion via CXCR2

CXCL5 has been reported to interact with CXCR2 receptor and promote the invasion in several cancer cells[23]. I examined whether CXCL5 could stimulate OSCC cell invasion through CXCR2. Treatment with 5 μg/ml anti-CXCR2 reduced cell invasion by 26%, 32%, 27%, and 31%, respectively and did not result in CXCL5-induced cell invasion in Ca9-22, YD-10B, HSC-2, and HSC-3 cells (Fig. 5).

Next, I detected that *CXCR2* mRNA expression was higher in Ca9-22 and YD-10B cells than in HSC-2 and HSC-3 cells (Fig. 6A). I established CXCR2 knockdown Ca9-22 and YD-10B cells using shRNA lentiviral particles and CXCR2 expression level in cell surface was quantified by flow cytometric analysis. Transfection with CXCR2 shRNA-1 and shRNA-4 reduced the expression level of CXCR2 by 35% and 27% in Ca9-22 cells (Fig. 6B) and 47% and 6% in YD-10B cells (Fig. 6C), respectively. Interestingly, notable morphological change into the typical cobblestone-like appearance was detected in CXCR2 knockdown cells, particularly in CXCR2 shRNA-1-transfected Ca9-22 (Fig. 7A) and YD-10B cells (Fig. 7B), compared to scrambled shRNA transfected cells. When CXCR2 knockdown cells were cultured for 24 h and 72 h, cell viability was significantly reduced by 9% and 20% in Ca9-22 cells (Fig. 7C) and by 17% and 26% in YD-10B cells (Fig. 7D), respectively. CXCR2 knockdown also significantly reduced Ca9-22 (Fig. 7E) and YD-10B cell invasion (Fig. 7F). CXCL5-stimulated cell invasion was not detected in CXCR2 knockdown Ca9-22 (Fig. 8A) and YD-10B cells (Fig. 8B). These results indicate that CXCR2 has a critical role

in OSCC cell invasion and CXCL5 promotes Ca9-22 and YD-10B cell invasion through CXCR2.

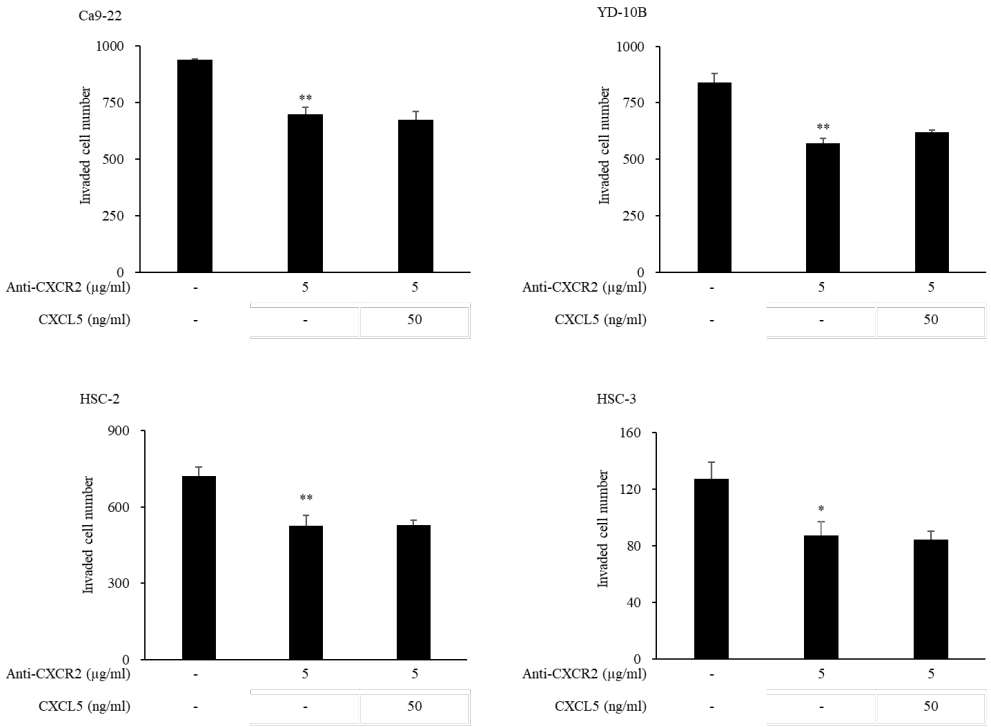

Figure 5. Treatment with anti-CXCR2 blocked CXCL5-stimulated OSCC cell invasion. Cell invasion was measured in Ca9-22, YD-10B, HSC-2, and HSC-3 cells treated with 50 ng/ml CXCL5 and/or 5 μg/ml anti-CXCR2. * $P < 0.05$, ** $P < 0.01$ versus untreated cells.

A

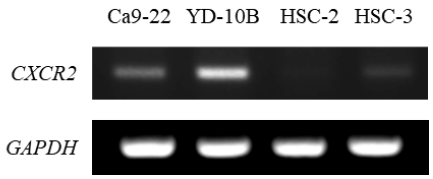

B

Wild type

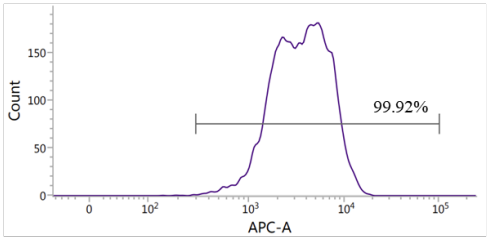

Scrambled shRNA

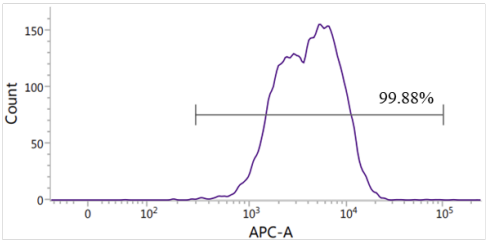

CXCR2 shRNA-1

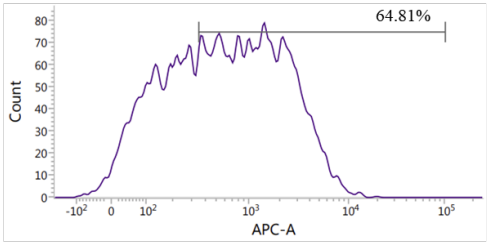

CXCR2 shRNA-2

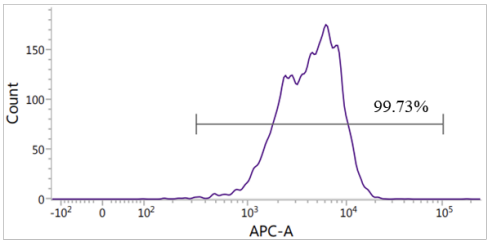

CXCR2 shRNA-4

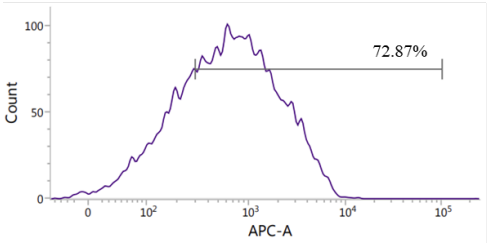

Cell type	CXCR2 expression level
	Ca9-22
Wild type	99.92%
Scrambled shRNA	99.88%
CXCR2 shRNA-1	64.81%
CXCR2 shRNA-2	99.73%
CXCR2 shRNA-4	72.87%

C

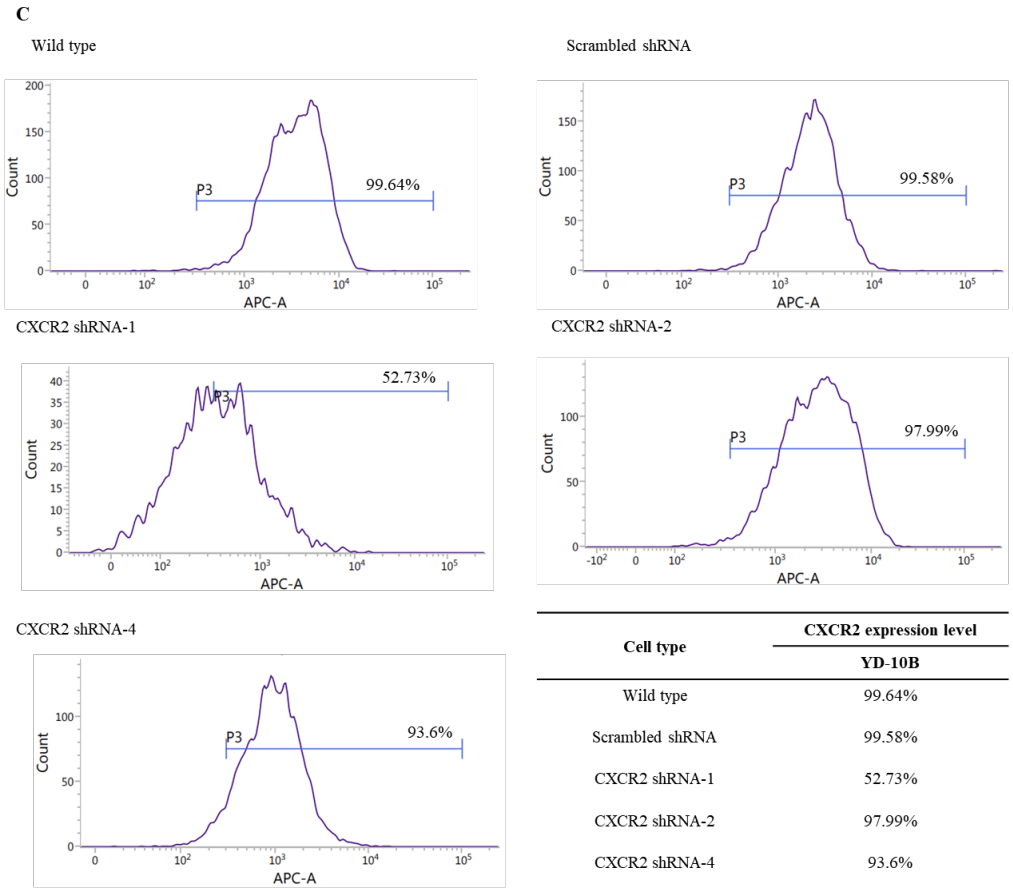

Cell type	CXCR2 expression level
	YD-10B
Wild type	99.64%
Scrambled shRNA	99.58%
CXCR2 shRNA-1	52.73%
CXCR2 shRNA-2	97.99%
CXCR2 shRNA-4	93.6%

Figure 6. CXCR2 was knockdowned in Ca9-22 and YD-10B OSCC cell lines. (A) CXCR2 mRNA expression level was measured in 4 OSCC cell lines. (B, C) Ca9-22 and YD-10B cells were transfected with scrambled and CXCR2 shRNAs. Wild-type and transfected cells were fixed and stained with primary anti-CXCR2 and secondary anti-APC antibody. CXCR2 level expressed in cell surface was detected by flow cytometric analysis in wild-type, scrambled, and CXCR2 shRNA-transfected (B) Ca9-22 and (C) YD-10B cells.

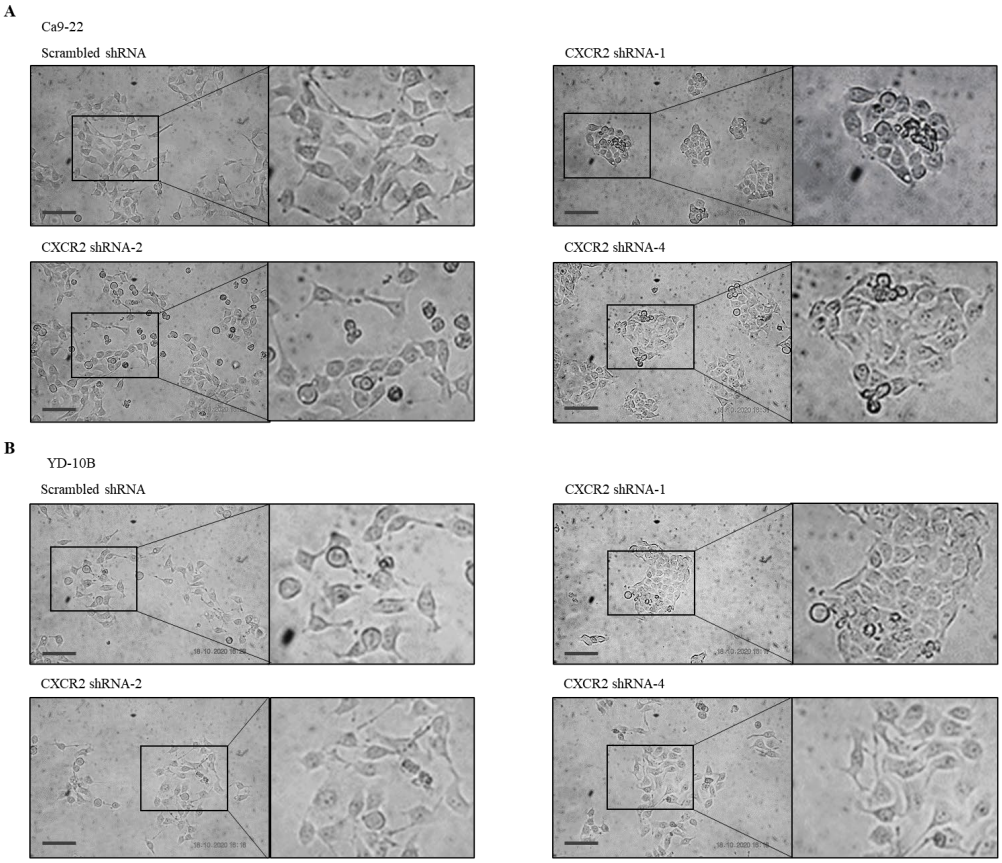

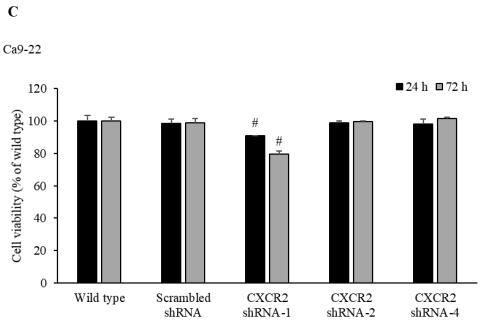

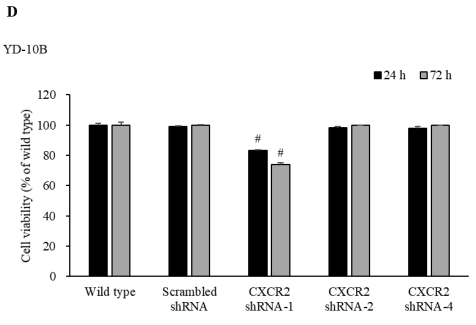

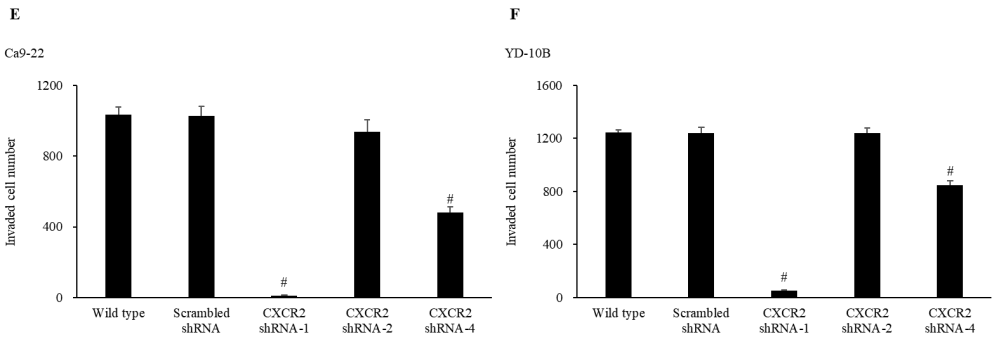

Figure 7. OSCC cell viability and invasion were inhibited by CXCR2 knockdown. (A, B) Cell morphology was observed in scrambled and CXCR2 shRNA-transfected (A) Ca9-22 and (B) YD-10B cells. Representative images were obtained at x40 magnification. (C, D) Wild-type, scrambled, and CXCR2 shRNA-transfected (C) Ca9-22 and (D) YD-10B cells were cultured for 24 h and 72 h and cell viability was measured by an MTT assay. (E, F) Cell invasion was measured using transwell chamber in wild-type, scrambled, and CXCR2 shRNA-transfected (E) Ca9-22 and (F) YD-10B cells. # $P < 0.001$ versus scrambled shRNA-transfected cells.

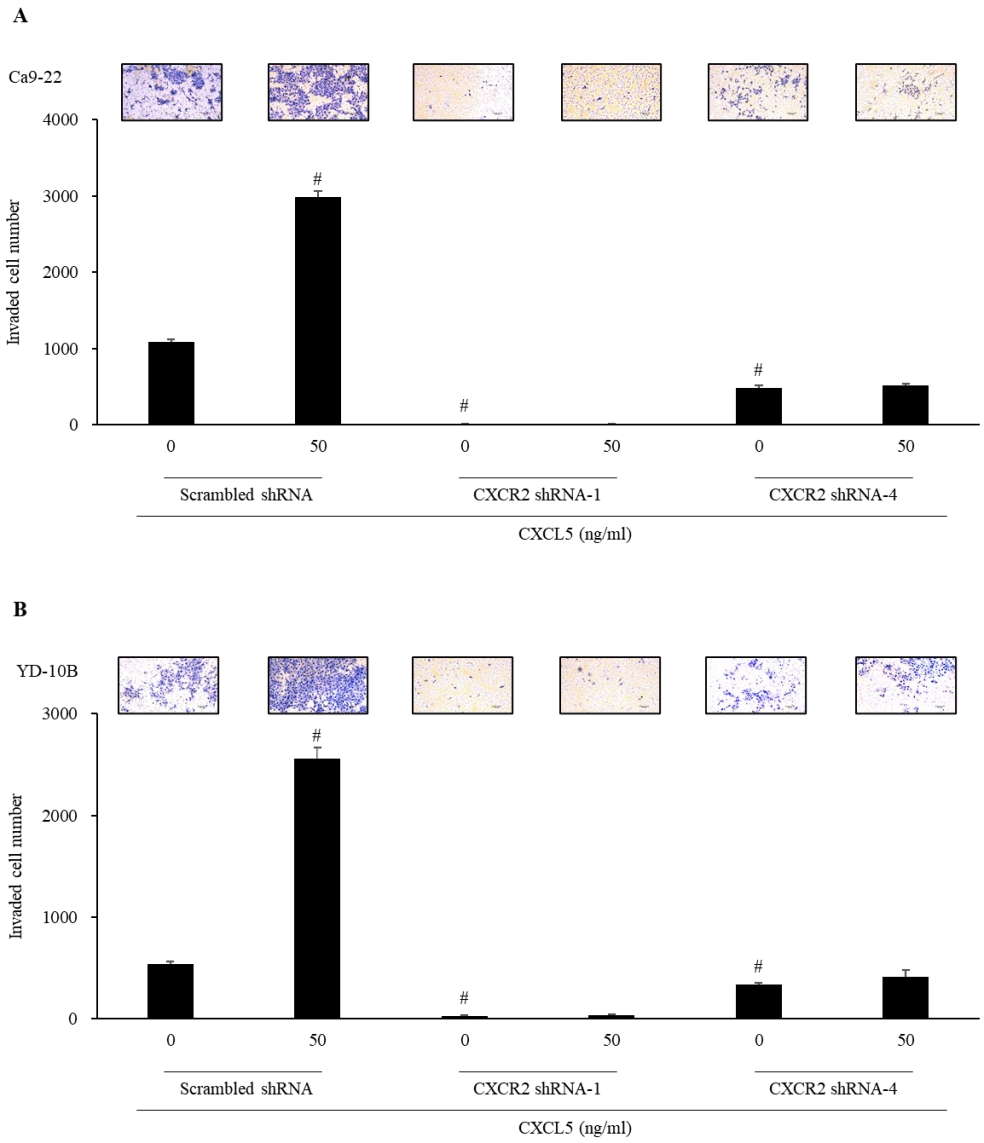

Figure 8. CXCR2 knockdown inhibited OSCC cell invasion in the absence or presence of CXCL5. Cell invasion was measured in scrambled or CXCR2 knockdown (A) Ca9-22 and (B) YD-10B cells in the absence or presence of CXCL5. # $P < 0.001$ versus scrambled shRNA-transfected cells.

3. CXCL5 stimulation upregulated interferon alpha response- and ROS-related genes in OSCC cells

To identify the target molecules activated by CXCL5 in OSCC cells, I performed transcriptome analysis with total RNA sequencing in Ca9-22 OSCC cells treated with CXCL5 for 6 h and 24 h. I carried out GSEA from RNA-seq data for finding general trends in the huge lists of genes. GSEA revealed that genes related to interferon alpha response and ROS pathway were enriched in CXCL5-treated Ca9-22 cells for 6 h (Fig. 9A) and 24 h (Fig. 9B), respectively.

4. CXCL5 stimulated transcriptional activation by NF-κB, HIF-1α, and AP-1 in OSCC cells

Next, forty-five different transcriptional activities were investigated in CXCL5-treated and CXCR2 knockdown Ca9-22 cells, using Cignal Finder 45-Reporter array. Transcriptional activities of octamer-binding transcription factor 4, serum response element/Elk-1, aryl hydrocarbon receptor, liver X receptors, STAT1/2, activator protein-1 (AP-1), HIF-1α, Krüppel-like factor 4, NF-κB, specificity protein 1, and CCAAT-enhancer-binding protein were increased in CXCL5-treated OSCC cells, but decreased in CXCR2 knockdown OSCC cells. Among several transcriptional activities upregulated by CXCL5 stimulation (Fig. 10A) and downregulated by CXCR2 knockdown (Fig. 10B), I focused on the changed transcriptional activities of NF-κB, HIF-1α, and AP-1. NF-κB, HIF-1α, and AP-1 are critical transcription factors to

regulate ROS pathway-related genes[42]. To confirm whether CXCL5 could activate NF-κB, I investigated the expression levels of the total and phosphorylated forms of p65 at serine 311 and IκBα at serine 32/36 in CXCL5-treated Ca9-22 and YD-10B cells. The expression levels of p-p65, p65, and IκBα were increased but the phosphorylation of IκBα was not. The increased level of p65 was detected in both cytosolic and nucleus fractions (Fig. 10C).

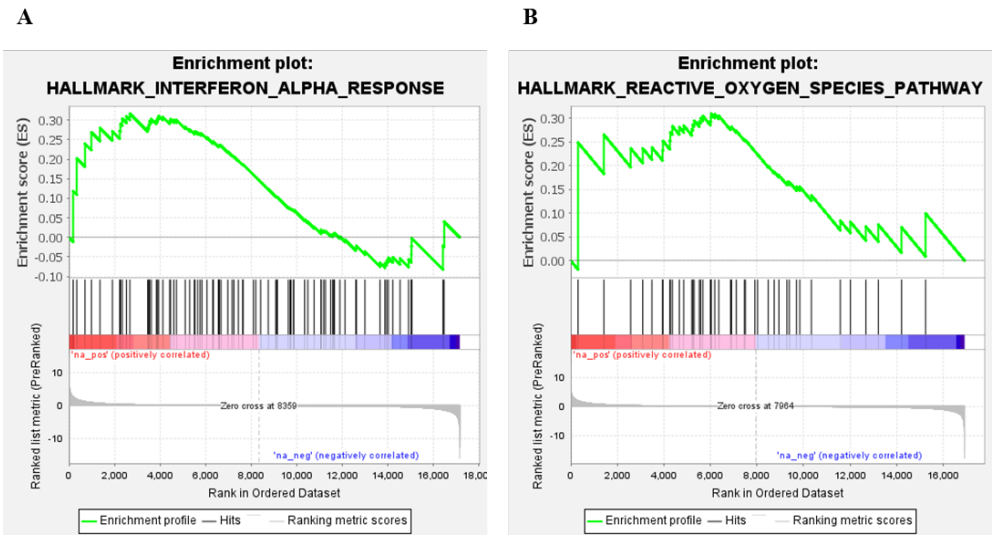

Figure 9. CXCL5 upregulated interferon alpha response- and ROS pathway-related genes. GSEA was performed using RNA-seq data. (A) Interferon alpha response-related and (B) ROS pathway-related gene sets were upregulated in Ca9-22 cells treated with 50 ng/ml CXCL5 for 6 h and 24 h, respectively.

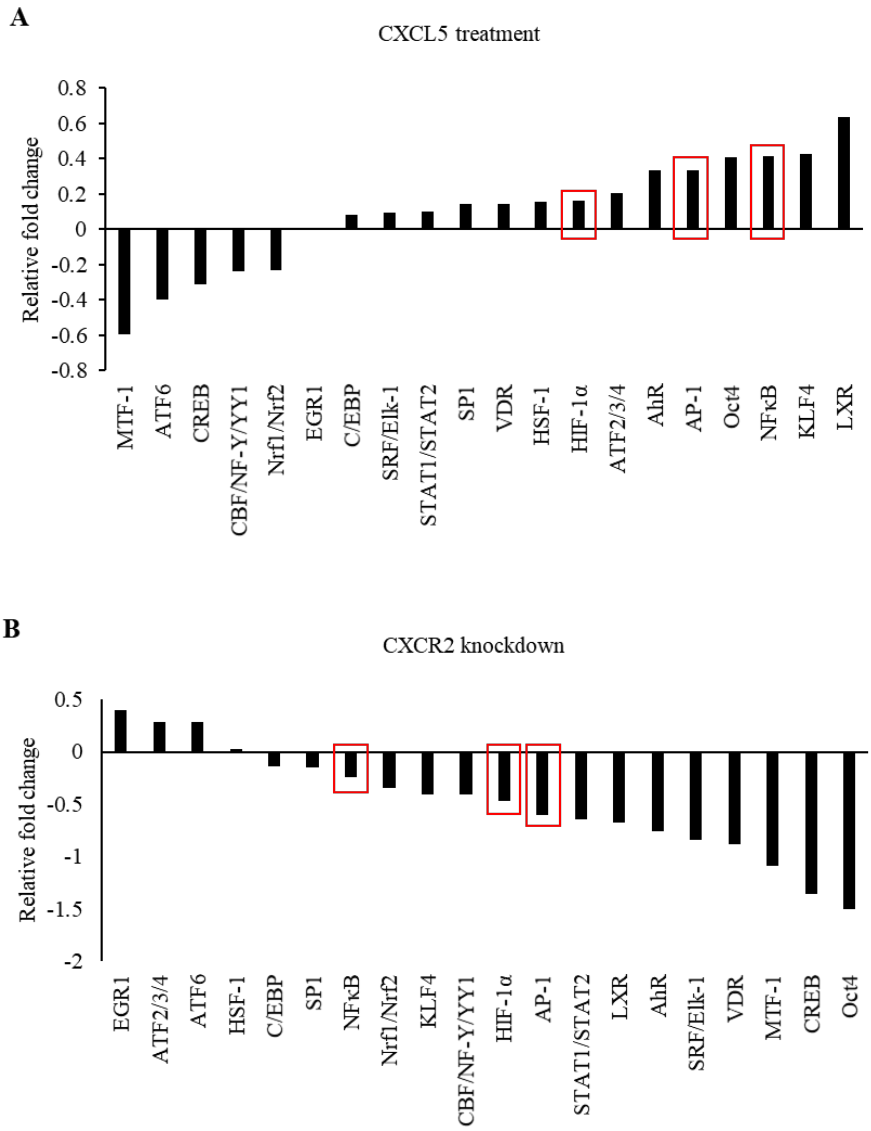

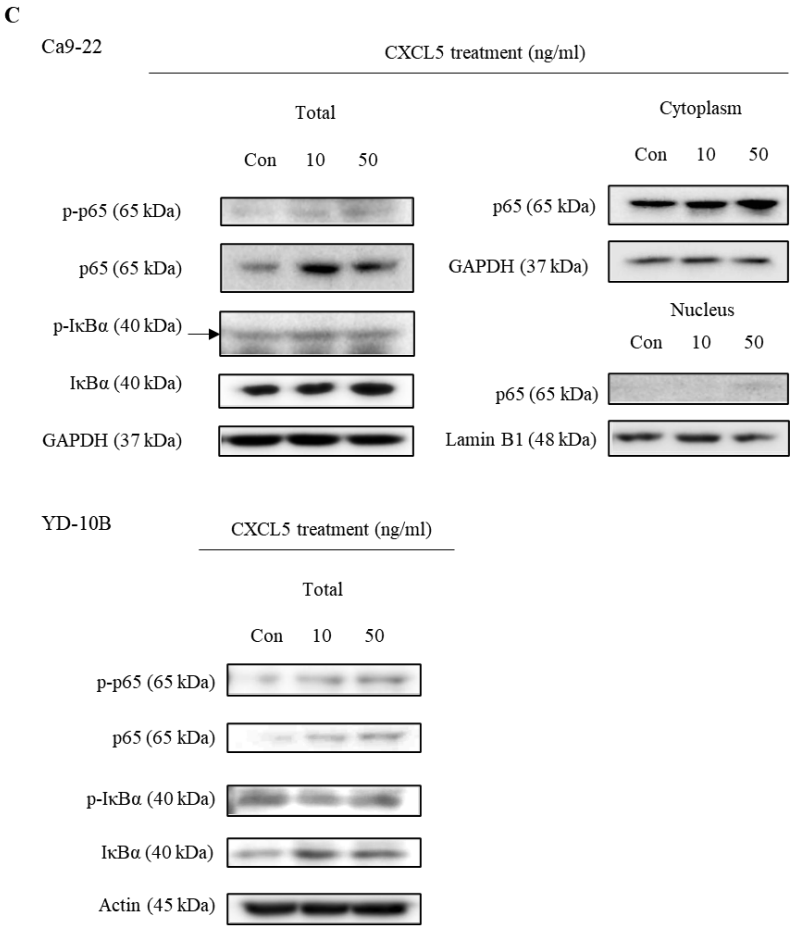

Figure 10. CXCL5 upregulated NF-κB, HIF-1α, and AP-1 transcriptional activities and the expression levels of p65 and IκBα. Forty-five different transcriptional activities were analyzed in (A) Ca9-22 cells treated with 50 ng/ml CXCL5 for 24 h and (B) CXCR2 knockdown Ca9-22 cells, using Cignal Finder 45-Pathway Reporter Array. The fold change in each transcriptional activity was calculated from the normalized luciferase activities in (A) CXCL5-treated versus untreated cells or (B) scrambled shRNA-transfected cells versus CXCR2 shRNA-

transfected cells. (C) Expression levels and cellular localization of p-p65 (Ser311), p65, p-IκBα (Ser32/36), and IκBα were measured in CXCL5-treated Ca9-22 and YD-10B cells ($1x10^5$ cells/dish) with Western blotting.

5. CXCL5 increased the invasion of OSCC cells by activating AKT and NF-κB via CXCR2

Atypical NF-κB signaling pathway that is independent of IκBα degradation has been known to mediate through ROS generation[43] or phosphorylated AKT at serine 473[44, 45]. ROS generation was not changed in CXCL5-treated Ca9-22 cells (Fig. 11A). However, AKT phosphorylation at serine 473 was increased by CXCL5 treatment in a dose-dependent manner in Ca9-22 and YD-10B cells (Fig. 11B). AKT phosphorylation at serine 473 and the expression levels of p-p65, p65, and IκBα were increased by treatment with CXCL5 in scrambled shRNA-transfected Ca9-22 cells, but not CXCR2 shRNA-1-transfected cells (Fig. 12). Treatment with NF-κB inhibitor JSH-23 or AKT inhibitor MK-2206 blocked the invasion of OSCC cells stimulated with CXCL5 or not (Fig. 13). Treatment with JSH-23 reduced CXCL5-induced expression levels of p65 and IκBα but CXCL5-induced AKT phosphorylation was not. Treatment with MK-2206 inhibited CXCL5-stimulated expression levels of p65, IκBα, and p-AKT(Fig.14). These results suggest that CXCL5 promotes the invasion by activating AKT and NF-κB via CXCR2 in OSCC cells.

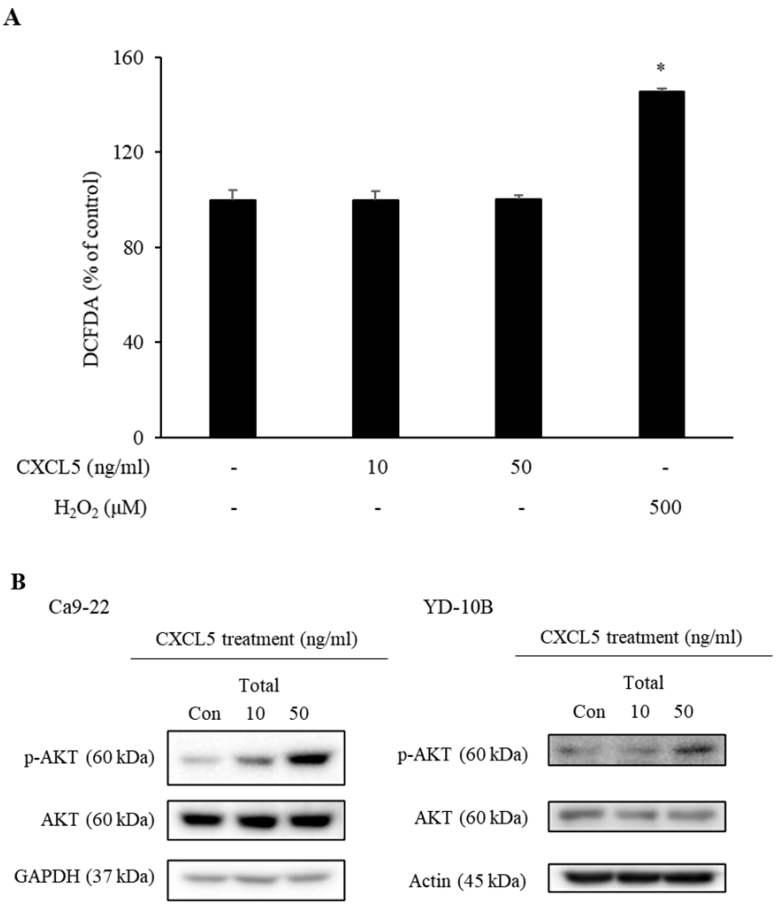

Figure 11. CXCL5 stimulation did not cause ROS production but activated AKT in OSCC cells. (A) ROS levels were measured by flow cytometry in DCFDA-stained Ca9-22 cells after treatment with CXCL5 for 24 h. (B) Expression levels of p-AKT (Ser473) and AKT were measured in CXCL5-treated Ca9-22 and YD-10B cells by Western blotting. * $P < 0.001$ versus untreated cells.

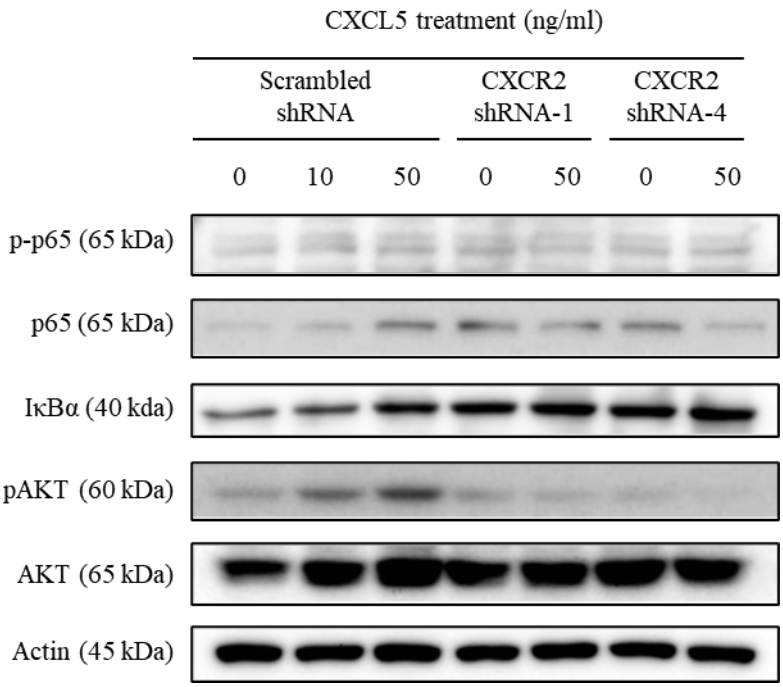

Figure 12. CXCL5/CXCR2 axis upregulated the expression levels of p-p65, p65, IκBα, and p-AKT. Scrambled shRNA- or CXCR2 shRNA-transfected cells were treated with CXCL5 at the indicated concentrations. The expression levels of p-p65 (Ser311), p65, IκBα, p-AKT (Ser473), and AKT were examined in the total cell lysate with Western blotting.

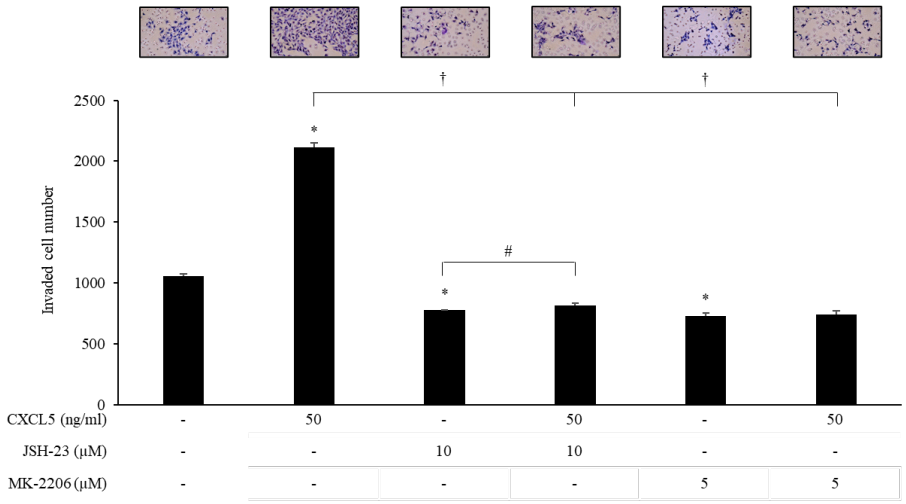

Figure 13. Treatment with inhibitors of NF-κB or AKT blocked CXCL5-stimulated invasion. Cell invasion was measured in Ca9-22 cells treated with 10 μM JSH-23 or 5 μM MK-2206 in the absence or presence of 50 ng/ml CXCL5. Representative images were obtained at x40 magnification. * $P < 0.001$ versus untreated cells, † $P < 0.001$ versus CXCL5 alone-treated cells, # $P < 0.001$ versus JSH-23-treated cells.

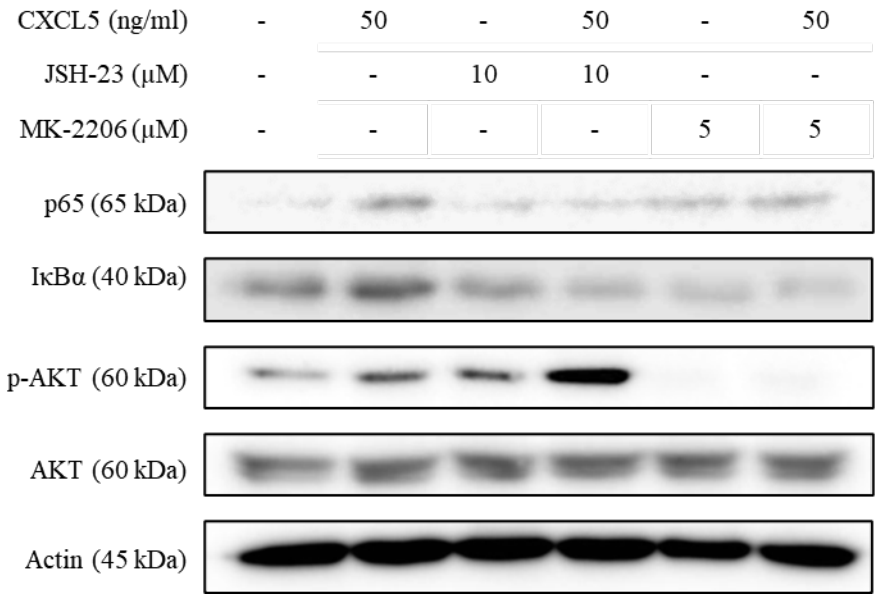

Figure 14. CXCL5-induced the expression levels of p65 and IκBα reduced by treatment with NF-κB or AKT inhibitor. Ca9-22 cells were treated with 50 ng/ml CXCL5 and/or 10 μM JSH-23 or 5 μM MK-2206 for 24 h. The expression levels of p65, IκBα, p-AKT, and AKT were detected by Western blotting.

6. CXCL5 is associated with poor prognosis in head and neck cancer patients

I investigated mRNA expression levels of *CXCL5* and *CXCR2* in cancer tissues compared with normal tissues by analyzing the ONCOMINE platform data. *CXCL5* was significantly overexpressed by 16-fold in head and neck cancer tissues in one dataset and *CXCR2* was downregulated by more than 2-fold in head and neck cancer tissues in 7 datasets (Fig. 15A and Table 1). In Kaplan-Meier survival analysis, overall survival showed a decreasing tendency in head and neck cancer patients with high expression level of *CXCL5* mRNA and an increasing tendency in patients with high *CXCR2* mRNA expression level (Fig. 15B). *CXCL5* gene expression was significantly higher in the most advance stage IV than in other stages. However, there was no correlation between *CXCR2* mRNA level and TNM stage in head and neck cancer patients (Fig. 15C).

In addition, analysis of TCGA head and neck cancer datasets showed that *CXCL5* mRNA expression was significantly associated with *NFKB1* and *IKBA* mRNA expressions and tends to increase in *RELA* mRNA expression (Fig. 16).

A

Analysis Type by Cancer	CXCL5 Total Unique Analysis	CXCL5 Cancer vs. Normal		CXCR2 Total Unique Analysis	CXCR2 Cancer vs. Normal	
Bladder Cancer	10			10		
Brain and CNS Cancer	29	1		30	2	3
Breast Cancer	39		7	39		
Cervial Cancer	10	1		10		3
Colorectal Cancer	33	10		33	2	
Esophageal Cancer	7			7		5
Gastric Cancer	20	1	1	20		
Head and Neck Cancer	32	1		32		7
Kidney Cancer	20	2	2	20		
Leukemia	25	1		27		5
Liver Cancer	10	1		10		
Lung Cancer	27		2	27		3
Lymphoma	30			33		
Melanoma	5	1	1	5		
Myeloma	8		1	8		
Other Cancer	31	3		31	3	2
Ovarian Cancer	14			14		
Pancreatic Cancer	11	5		11		1
Prostate Cancer	15			15		
Sarcoma	20	1	3	20	1	2
Significant Unique Analysis		28	17		8	31
Total Unique Analysis		392			398	

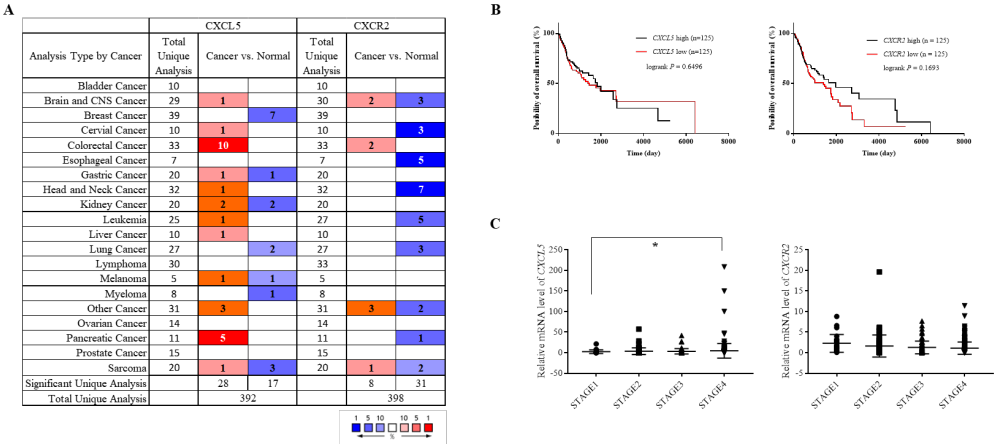

Figure 15. CXCL5 mRNA expression is correlated with poor prognosis in patients with head and neck cancer. (A) The comparison showed the number of datasets with the mRNA expression of *CXCL5* and *CXCR2* in head and neck cancer patients. Cut-off of P-value and fold change were as following: P-value < 0.01, fold change = 2, and gene rank = top 10% in cancer versus normal tissues. (B) Kaplan-Meier survival analysis indicated the association of *CXCL5* or *CXCR2* mRNA expression with overall survival of head and neck cancer patients. (C) Relative mRNA expression of *CXCL5* or *CXCR2* according to TNM stage was examined from the TCGA database. * P < 0.001 versus STAGE1 *CXCL5* mRNA level.

Table 1. The transcription levels of CXCL5 and CXCR2 between head and neck cancer patients and normal samples in ONCOMINE database.

Gene ID	Cohort	Data type	Sample (n)	Fold-change	P-value
CXCL5	Ginos Head-Neck	mRNA	Head and Neck Squamous Cell Carcinoma (41) vs. Normal (13)	16.431	7.42E-11
CXCR2	Peng Head-Neck	mRNA	Oral Cavity Squamous Cell Carcinoma (57) vs. Normal (22)	-3.914	9.01E-23
	Ginos Head-Neck	mRNA	Head and Neck Squamous Cell Carcinoma (41) vs. Normal (13)	-7.121	4.33E-18
	Pyeon Multi-cancer	mRNA	Tongue Carcinoma (15) vs. Normal (22)	-2.247	1.01E-05
		mRNA	Oral Cavity Carcinoma (4) vs. Normal (22)	-3.325	1.09E-05
		mRNA	Tonsillar Carcinoma (6) vs. Normal (22)	-2.038	3.00E-03
	Schlingemann Head-Neck	mRNA	Hypopharyngeal Squamous Cell Carcinoma (4) vs. Noraml (4)	-3.546	5.00E-03
	Cromer Head-Neck	mRNA	Head and Neck Squamous Cell Carcinoma (34) vs. Normal (4)	-4.432	2.00E-03
TCGA, The Cancer Genome Atlas					

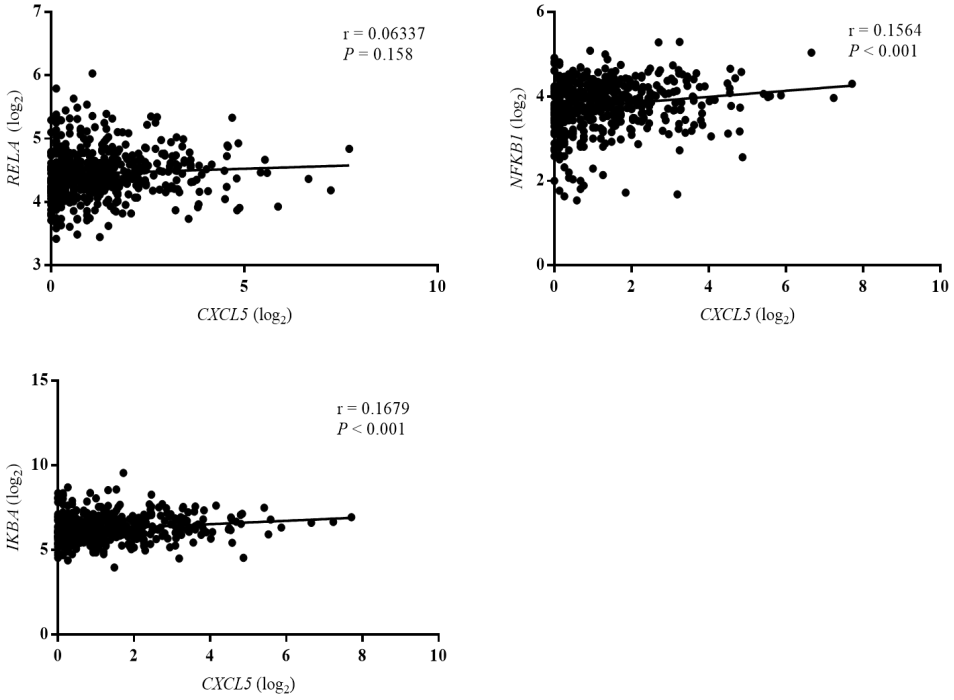

Figure 16. Oncogenic effect of CXCL5 was associated with NF-κB in patients with head and neck cancer by Pearson's correlation analysis. The mRNA-seq data were retrieved from TCGA and the Pearson's correlation analysis was employed to determine the correlation between *CXCL5* and target mRNAs (*RELA*, *NFKB*, and *IKBA*). Scatter plots represent normalized FPKM values for each gene. r: Pearson's correlation coefficient.

Ⅳ. Discussion

Surgical resection combined with radiotherapy and chemotherapy is the classical treatment for oral cancer. Despite the improved treatment for oral cancer, OSCC is still a challenging disease to treat[2]. Targeting oncogenic proteins associated with OSCC development is increasingly considered a promising strategy to cure OSCC. Bone invasion is a critical factor in determining the prognosis of oral cancer patients[5, 6]. Therefore, identifying the molecular mechanism that could modulate cancer invasion and tumor microenvironment is expected to improve the treatment efficacy of OSCC and guide molecular targeted therapy. CXCL5 is the chemokine that is overexpressed in 14 different tumor types and stimulates cancer cell invasion and proliferation[23]. CXCL5 secretes into tumor microenvironment from cancer cells and cancer-associated stromal cells and is correlated with negative prognosis[19-24, 46]. I determined the role of CXCL5 in OSCC invasion and underlying molecular mechanism.

I first found that CXCL5 treatment promoted OSCC cell viability and invasion and neutralizing CXCL5 with anti-CXCL5 inhibited OSCC cell invasion. CXCR2 has been reported as the only receptor of CXCR5 and to be responsible for CXCL5-mediated breast, prostate, and lung cancer cell metastasis[23, 46]. In this study, CXCR2 knockdown OSCC cells indicated remarkable transition to cobblestone morphology with tight cell-cell adhesion. This morphology is accepted as one of less metastatic characteristics[47]. Neutralization of CXCR2 with its specific antibody and CXCR2

knockdown with shRNA effectively inhibited OSCC cell invasion in the absence or presence of CXCL5. These results indicate that CXCL5 and its receptor CXCR2 have critical roles in OSCC cell invasion.

CXCL5 activates multiple signaling pathways, including mitogen-activated protein kinase kinase (MEK)/ERK, PI3K/AKT/NF-κB, JAK/STAT, MSK1/Elk-1, and Egr-1/cdk4, and promotes the proliferation, migration, and invasion of cancer cells[23, 48]. I investigated CXCL5-regulated target molecules in OSCC cells. In GSEA analysis on the RNA-seq transcriptome analysis data, interferon alpha response-related and ROS pathway-related genes were enriched in CXCL5-treated OSCC cells. In Cignal Finder 45-Pathway Reporter array, I detected that the transcriptional activities of NF-κB, HIF-1α, and AP-1 were upregulated in CXCL5-treated OSCC cells and downregulated by CXCR2 knockdown. These transcription factors have been reported to regulate the expression of genes involved in interferon alpha response[49-51] and ROS pathway[52-54] and I first studied molecular mechanism by which CXCL5 activates NF-κB and promotes cell invasion in OSCC cells.

In the canonical NF-κB pathway, the degradation of IκBα is primarily triggered through its phosphorylation at two N-terminal serines by a multi-subunit IκB kinase (IKK) complex, resulting in rapid and transient nuclear translocation of canonical NF-κB members of predominantly the p50/p65 and p50/c-Rel dimers[55, 56]. The noncanonical NF-κB activation relies on processing of the NF-κB2 precursor protein, p100, resulting in generation of mature NF-κB2 p52 and nuclear translocation of NF-

κB complex p52/RelB[57, 58]. In the atypical pathway, IκBα is phosphorylated on Tyr 42 and p50/p65 NF-κB may be activated without proteasomal degradation of IκBα[59, 60]. Atypical NF-κB signaling pathway is induced by ROS pathway[43] or PI3K/AKT[44, 45]. It has been reported that CXCL5/CXCR2 signaling pathway induced activation of NF-κB in colorectal[61] and pancreatic[62] cancer cells, but the NF-κB transcriptional regulation system is not fully understood. In this study, CXCL5 treatment increased the levels of p65 NF-κB subunit, p-p65, and nuclear p65 levels in OSCC cells. Because the accumulated IκBα level was detected, I investigated whether CXCL5 stimulation could activate NF-κB without proteasomal degradation of IκBα. ROS production or AKT activation cause the phosphorylation on Tyr 42 of IκBα pathway[43-45]. I found that CXCL5 treatment induced AKT phosphorylation on Ser 473 but did not cause ROS generation.

I further confirmed whether CXCL5 transduces signaling via CXCR2. CXCL5-induced activation of p65 NF-κB and AKT was not observed in CXCR2 knockdown OSCC cells. Treatment with NF-κB or AKT inhibitor significantly inhibited the invasion of OSCC cells stimulated with CXCL5 or not. CXCL5-induced expression levels of p65 NF-κB and IκBα were inhibited by NF-κB and AKT inhibitors, but AKT phosphorylation was not blocked by NF-κB inhibitor. These findings indicate that CXCL5 promotes OSCC cell invasion by activating AKT/NF-κB pathway via its receptor CXCR2.

In bioinformatics analysis from TCGA datasets, *CXCL5* has positive correlation with

NFKB1 and *IKBA*. In addition, the overexpression of *CXCL5* was observed in oral cancer patients compared to normal tissue and associated with poor prognosis.

In conclusion, CXCL5 stimulates OSCC cell invasion through the AKT phosphorylation and NF-κB signaling pathway via CXCR2. Thus, CXCL5/CXCR2 and their downstream target molecules may be effective candidate markers for OSCC cell invasion.

Ⅴ. Conclusions

In summary, CXCL5 increased the survival and invasion of OSCC cells. Neutralization and knockdown of CXCR2 inhibited the invasion of OSCC cells in the absence or presence of CXCL5. CXCL5 upregulated genes participating in the interferon alpha response and reactive oxygen species pathway and activated the transcriptional activity of NF-κB, HIF-1α, and AP-1. CXCL5/CXCR2 signaling pathway induced OSCC cell invasion and expression of NF-κB and IκBα through the activation of AKT/NF-κB. *CXCL5* is correlated with poor prognosis and higher expression of *NFBK1* and *IKBA* in oral cancer patients.

Taken together, CXCL5/CXCR2 and their downstream target molecules serve as a biomarker for predicting the potential for invasion in oral cancer patients.

References

1. César Rivera. Essentials of oral cancer. International Journal of Clinical and Experimental Pathology. 2015 Sep 1;8(9):11884-94.
2. Daniel E. Johnson, Barbara Burtness, C René Leemans, Vivian Wai Yan Lui, Julie E Bauman, Jennifer R Grandis. Head and neck squamous cell carcinoma. Nature Reviews Disease Primers. 2020 Nov 26;6(1):92.
3. Amr Bugshan, Imran Farooq. Oral squamous cell carcinoma: metastasis, potentially associated malignant disorders, etiology and recent advancements in diagnosis. F1000Research. 2020 Apr 2;9:229.
4. Rebecca L Siegel, Kimberly D Miller, Hannah E Fuchs, Ahmedin Jemal. Cancer Statistics, 2021. CA: A Cancer Journal for Clinicians. 2021 Jan 12;71(1):7-33.
5. Adel K El-Naggar, John K C Chan, Takashi Takata, Jennifer R Grandis, Pieter J Slootweg. The fourth edition of the head and neck World Health Organization blue book: editors' perspectives. Human Pathology. 2017 Aug;66:10-12.
6. Eijiro Jimi, Hiroyuki Furuta, Kou Matsuo, Kazuhiro Tominaga, Tetsu Takahashi, Osamu Nakanishi. The cellular and molecular mechanisms of bone invasion by oral squamous cell carcinoma. Oral Diseases. 2011 Jul;17(5):462-8.
7. Seba Abraham, Bhagyalekshmi Mallika, Arunima Reshma, ReejaMol Mohammed Kassim. An Atypical Case of Oral Squamous Cell Carcinoma of Mandibular Alveolus. Case Reports in Dentistry. 2019 Nov 13;2019:2521685.

8. Daniella Karassawa Zanoni, Snehal G Patel, Jatin P Shah. Changes in the 8th Edition of the American Joint Committee on Cancer (AJCC) Staging of Head and Neck Cancer: Rationale and Implications. Current Oncology Reports. 2019 Apr 17;21(6):52.

9. William M Lydiatt, Snehal G Patel, Brian O'Sullivan, Margaret S Brandwein, John A Ridge, Jocelyn C Migliacci, Ashley M Loomis, Jatin P Shah. Head and Neck cancers-major changes in the American Joint Committee on cancer eighth edition cancer staging manual. CA: A Cancer Journal for Clinicians. 2017 Mar;67(2):122-137.

10. Rinaldo Florencio-Silva, Gisela Rodrigues da Silva Sasso, Estela Sasso-Cerri, Manuel Jesus Simões, Paulo Sérgio Cerri. Biology of Bone Tissue: Structure, Function, and Factors That Influence Bone Cells. BioMed Research International. 2015;2015:421746.

11. Mojtaba Ansari. Bone tissue regeneration: biology, strategies and interface studies. Progress in Biomaterials. 2019 Dec;8(4):223-237.

12. Jingjing Quan, Yuluan Hou, Weiling Long, Shu Ye, Zhiyuan Wang. Characterization of different osteoclast phenotypes in the progression of bone invasion by oral squamous cell carcinoma. Oncology Reports. 2018 Mar;39(3):1043–1051.

13. Victor R Preedy, Vinood B Patel. Macrophage Inflammatory Protein-1 Alpha (MIP-1 alpha)/CCL3: As a Biomarker. General Methods in Biomarker Research

and their Applications. 2015 June:223–249.

14. Yuki Takayama, Taisuke Mori, Takeshi Nomura, Takahiko Shibahara, Michiie Sakamoto. Parathyroid-related protein plays a critical role in bone invasion by oral squamous cell carcinoma. International Journal of Oncology. 2010 Jun;36(6):1387-94.
15. Kou Kayamori, Kei Sakamoto, Tomoki Nakashima, Hiroshi Takayanagi, Kei-Ichi Morita, Ken Omura, Su Tien Nguyen, Yoshio Miki, Tadahiro Iimura, Akiko Himeno, Takumi Akashi, Hisafumi Yamada-Okabe, Etsuro Ogata, Akira Yamaguchi. Roles of interleukin-6 and parathyroid hormone-related peptide in osteoclast formation associated with oral cancers: significance of interleukin-6 synthesized by stromal cells in response to cancer cells. The American Journal of Pathology. 2010 Feb;176(2):968-80.
16. Yuvaraj Sambandam, Purushoth Ethiraj, Jessica D Hathaway-Schrader, Chad M Novince, Ezhil Panneerselvam, Kumaran Sundaram, Sakamuri V Reddy. Autoregulation of RANK ligand in oral squamous cell carcinoma tumor cells. Journal of Cell Physiology. 2018 Aug;233(8):6125-6134.
17. Nianhui Cui, Takeshi Nomura, Nobuo Takano, Enbo Wang, Wei Zhang, Takeshi Onda, Takahiko Shibahara. Osteoclast-related cytokines from biopsy specimens predict mandibular invasion by oral squamous cell carcinoma. Experimental and Therapeutic Medicine. 2010 Sep;1(5):755–760.
18. Yu Ling Hsu, Mei Fang Hou, Pao Lin Kuo, Yu Fen Huang, Eing Mei Tsai.

Breast tumor-associated osteoblast-derived CXCL5 increases cancer progression by ERK/MSK1/Elk-1/snail signaling pathway. Oncogene. 2013 Sep 12;32(37):4436-47.

19. Ricardo Romero-Moreno, Kimberly J Curtis, Thomas R Coughlin, Maria Cristina Miranda-Vergara, Shourik Dutta, Aishwarya Natarajan. The CXCL5/CXCR2 axis is sufficient to promote breast cancer colonization during bone metastasis. Nature Communications. 2019 Sep 27;10(1):4404.
20. Hernan Roca, Jacqueline D Jones, Marta C Purica, Savannah Weidner, Amy J Koh, Robert Kuo, John E Wilkinson, Yugang Wang, Stephanie Daignault-Newton, Kenneth J Pienta, Todd M Morgan, Evan T Keller, Jacques E Nör, Lonnie D Shea, Laurie K McCauley. Apoptosis-induced CXCL5 accelerates inflammation and growth of prostate tumor metastases in bone. The Journal of Clinical Investigation. 2018 Jan 2;128(1):248-266.
21. Lesa A Begley, Sathish Kasina, Rohit Mehra, Shreelekha Adsule, Andrew J Admon, Robert J Lonigro, Arul M Chinnaiyan, Jill A Macoska. CXCL5 promotes prostate cancer progression. Neoplasia. 2008 Mar;10(3):244-54.
22. Lin Wang, Lin Shi, Jie Gu, Cheng Zhan, Junjie Xi, Jianyong Ding, Di Ge. CXCL5 regulation of proliferation and migration in human non-small cell lung cancer cells. Journal of Physiology and Biochemistry. 2018 May;74(2):313-324.
23. Yuan Cheng, XueLei Ma, Yu-Quan Wei, Xia-Wei Wei. Potential roles and targeted therapy of the CXCLs/CXCR2 axis in cancer and inflammatory diseases.

Biochimica et Biophysica Acta. Reviews on Cancer. 2019 Apr;1871(2):289-312.

24. Zhijun Zhou, Guanggai Xia, Zhen Xiang, Mingyang Liu, Zhewei Wei, Jie Yan, Wei Chen, Jintao Zhu, Niranjan Awasthi, Xiaotian Sun, Kar-Ming Fung, Yulong He, Min Li, Changhua Zhang. A C-X-C Chemokine Receptor Type 2-Dominated Cross-talk between Tumor Cells and Macrophages Drives Gastric Cancer Metastasis. Clinical Cancer Research. 2019 Jun 1;25(11):3317-3328.

25. Dong Cui, Yongfu Zhao, Jingchao Xu. Activated CXCL5-CXCR2 axis promotes the migration, invasion and EMT of papillary thyroid carcinoma cells via modulation of β-catenin pathway. Biochimie. 2018 May;148:1-11.

26. Wen-Ze Qiu, Hai-Bo Zhang, Wei-Xiong Xia, Liang-Ru Ke, Jing Yang, Ya-Hui Yu, Hu Liang, Xin-Jun Huang, Guo-Ying Liu, Wang-Zhong Li, Yan-Qun Xiang, Tie-Bang Kang, Xiang Guo, Xing Lv. The CXCL5/CXCR2 axis contributes to the epithelial-mesenchymal transition of nasopharyngeal carcinoma cells by activating ERK/GSK-3β/snail signalling. Journal of Experimental & Clinical Cancer Research. 2018 Apr 17;37(1):85

27. Agnes Forsthuber, Katharina Lipp, Liisa Andersen, Stefanie Ebersberger, 'Osvaldo Graña-Castro, Wilfried Ellmeier, Peter Petzelbauer, Beate M Lichtenberger, Robert Loewe. CXCL5 as Regulator of Neutrophil Function in Cutaneous Melanoma. The Journal of Investigative Dermatology. 2019 Jan;139(1):186-194.

28. Jingyi Liu, Pengnian Charles Lin, Binhua P Zhou. Inflammation Fuels Tumor

Progress and Metastasis. Current Pharmaceutical Design. 2015;21(21):3032–40

29. Sarah R Pickens, Nathan D Chamberlain, Michael V Volin, Mark Gonzalez, Richard M Pope, Arthur M Mandelin 2nd, Jay K Kolls, Shiva Shahrara. Anti-CXCL5 therapy ameliorates IL-17-induced arthritis by decreasing joint vascularization. Angiogenesis. 2011 Dec;14(4):443-55.
30. Lin-Yu Wang, Yi-Fang Tu, Yung-Chieh Lin, Chao-Ching Huang. CXCL5 signaling is a shared pathway of neuroinflammation and blood-brain barrier injury contributing to white matter injury in the immature brain. Journal of Neuroinflammation. 2016 Jan 6;13:6.
31. Jun Chen, Luqi Dai, Tao Wang, Junyun He, Yashu Wang, Fuqiang Wen. The elevated CXCL5 levels in circulation are associated with lung function decline in COPD patients and cigarette smoking-induced mouse model of COPD. Annals of Medicine. Aug-Sep 2019;51(5-6):314-329.
32. Kumaran Sundaram, D Sudhaker Rao, William L Ries, Sakamuri V Reddy. CXCL5 stimulation of RANK ligand expression in Paget's disease of bone. Laboratory Investigation. 2013 Apr;93(4):472-9.
33. Yong Qian, Yu Wang, Duan-Shu Li, Yong-Xue Zhu, Zhong-Wu Lu, Qing-Hai Ji, Gong Yang. The chemokine receptor-CXCR2 plays a critical role in the invasion and metastases of oral squamous cell carcinoma in vitro and in vivo. Journal of Oral Pathology & Medicine. 2014 Oct;43(9):658-66.

34. Lin Meng, Yueqi Zhao, Wenhuan Bu, Xing Li, Xinchen Liu, Dabo Zhou, Yumeng Chen, Shize Zheng, Quan Lin, Qilin Liu, Hongchen Sun. Bone mesenchymal stem cells are recruited via CXCL8-CXCR2 and promote EMT through TGF-β signal pathways in oral squamous carcinoma. Cell Proliferation. 2020 Aug;53(8):e12859.

35. Eun Kyoung Kim, Sook Moon, Do Kyeong Kim, Xianglan Zhang, Jin Kim. CXCL1 induces senescence of cancer-associated fibroblasts via autocrine loops in oral squamous cell carcinoma. PLoS One. 2018 Jan 23;13(1):e0188847.

36. Döne Onan, Elizabeth H Allan, Julian M W Quinn, Jonathan H Gooi, Sueli Pompolo, Natalie A Sims, Matthew T Gillespie, T John Martin. The chemokine Cxcl1 is a novel target gene of parathyroid hormone (PTH)/PTH-related protein in committed osteoblasts. Endocrinology. 2009 May;150(5):2244-53.

37. Aimalie L Hardaway, Mackenzie K Herroon, Erandi Rajagurubandara, Izabela Podgorski. Marrow adipocyte-derived CXCL1 and CXCL2 contribute to osteolysis in metastatic prostate cancer. Clinical & Experimental Metastasis. 2015 Apr;32(4):353-68.

38. Janak L Pathak, Astrid D Bakker, Patrick Verschueren, Willem F Lems, Frank P Luyten, Jenneke Klein-Nulend, Nathalie Bravenboer. CXCL8 and CCL20 Enhance Osteoclastogenesis via Modulation of Cytokine Production by Human Primary Osteoblasts. PLoS One. 2015;10(6):e0131041.

39. Tony J Collins. ImageJ for microscopy. Biotechniques. 2007 Jul;43(1 Suppl):25-

30.

40. Aravind Subramanian, Pablo Tamayo, Vamsi K Mootha, Sayan Mukherjee, Benjamin L Ebert, Michael A Gillette, Amanda Paulovich, Scott L Pomeroy, Todd R Golub, Eric S Lander, Jill P Mesirov. Gene set enrichment analysis: a knowledge-based approach for interpreting genome-wide expression profiles. Proceedings of the National Academy of Sciences of the United States of America. 2005 Oct 25;102(43):15545-50.
41. Chong-Feng Gao, Qian Xie, Yan-Li Su, Julie Koeman, Sok Kean Khoo, Margaret Gustafson, Beatrice S Knudsen, Rick Hay, Nariyoshi Shinomiya, George F Vande Woude. Proliferation and invasion: plasticity in tumor cells. Proceedings of the National Academy of Sciences of the United States of America. 2005 Jul 26;102(30):10528-33.
42. John D Haye, Albena T Dinkova-Kostova, Kenneth D Tew. Oxidative Stress in Cancer. Cancer Cell. 2020 Aug 10;38(2):167-197.
43. Won Seok Yang, Jang Won Seo, Nam Jeong Han, Jung Choi, Ki-Up Lee, Hanjong Ahn, Sang Koo Lee, Su-Kil Park. High glucose-induced NF-kappaB activation occurs via tyrosine phosphorylation of IkappaBalpha in human glomerular endothelial cells: involvement of Syk tyrosine kinase. American Journal of Physiology. Renal Physiol. 2008 May;294(5):F1065-75.
44. Hao-Ling Sun, Ying-Na Liu, Yu-TIng Huang, Shin-Liang Pan, Dean Y Huang, Jin-Hwa Guh, Fei Yee Lee, Shu-Chun Kuo, Che-Ming Teng. YC-1 inhibits HIF-1

expression in prostate cancer cells: contribution of Akt/NF-kappaB signaling to HIF-1alpha accumulation during hypoxia. Oncogene. 2007 Jun 7;26(27):3941-51.

45. Alebert C Koong, Eunice Y Chen, Amato J Giaccia. Hypoxia causes the activation of nuclear factor kappa B through the phosphorylation of I kappa B alpha on tyrosine residues. Cancer Research. 1994 Mar 15;54(6):1425-30.

46. Wen Zhang, Huishan Wang, Mingyang Sun, Xueting Deng, Xueru Wu, Yilan Ma, Mengjing Li, Said Maisam Shuoa, Qiang You,corresponding author, Lin Miaocorresponding author. CXCL5/CXCR2 axis in tumor microenvironment as potential diagnostic biomarker and therapeutic target. Cancer Communications. 2020 Mar;40(2-3):69-80.

47. Lilia A Chtcheglova, Andreas Ohlmann, Danila Boytsov, Peter Hinterdorfer, Siegfried G Priglinger, Claudia S Priglinger. Nanoscopic Approach to Study the Early Stages of Epithelial to Mesenchymal Transition (EMT) of Human Retinal Pigment Epithelial (RPE) Cells In Vitro. Life. 2020 Jul 30;10(8):128.

48. Jinglin Xia, Xiaojing Xu, Peixin Huang, Mingyan He, Xiangdong Wang. The potential of CXCL5 as a target for liver cancer - what do we know so far? Expert Opinion on Therapeutic Targets. 2015 Feb;19(2):141-6.

49. Lawrence M Pfeffer. The Role of Nuclear Factor κB in the Interferon Response. Journal of Interferon & Cytokine Research. 2011 Jul;31(7):553–559.

50. Scott A Gerber, Jordan S Pober. IFN-α Induces Transcription of Hypoxia-Inducible Factor-1α to Inhibit Proliferation of Human Endothelial Cells. Journal of

Immunology. 2008 Jul 15;181(2):1052–1062.

51. David E Levy, Isabelle Marié, Eric Smith, Arun Prakash. Enhancement and diversification of IFN induction by IRF-7-mediated positive feedback. Journal of Interferon & Cytokine Research. 2002 Jan;22(1):87-93.

52. Michael J Morgan, Zheng-gang Liu. Crosstalk of reactive oxygen species and NF-κB signaling. Cell Research. 2011 Jan;21(1):103–115.

53. Shahrzad Movafagh, Sean Crook, Kim Vo. Regulation of hypoxia-inducible factor-1a by reactive oxygen species: new developments in an old debate. Journal of Cellular Biochemistry. 2015 May;116(5):696-703.

54. Victor J Thannickal, Barry L Fanburg. Reactive oxygen species in cell signaling. American Journal of Physiology. Lung Cellular and Molecular Physiology. 2000 Dec;279(6):L1005-28.

55. Sören Beinke, Steven C Ley. Functions of NF-kappaB1 and NF-kappaB2 in immune cell biology. The Biochemical Journal 2004 Sep 1;382(Pt 2):393–409.

56. Michael Karin, Mireille Delhase. The I kappa B kinase (IKK) and NF-kappa B: key elements of proinflammatory signalling. Seminars in Immunology 2000 Feb;12(1):85–98.

57. Shao-Cong Sun. Non-canonical NF-kappaB signaling pathway. Cell Research 2011 Jan;21(1):71–85.

58. Shao-Cong Sun. The noncanonical NF-kappaB pathway. Immunological Reviews 2012 Mar;246(1):125–140.

59. Véronique Imbert, Rudolf A Rupec, Antonia Livolsi, Heike L Pahl, E.Britta-Mareen Traenckner, Christoph Mueller-Dieckmann, Dariush Farahifar, Bernard Rossi, Patrick Auberger, Patrick ABaeuerle, Jean-François Peyron. Tyrosine phosphorylation of I kappa B-alpha activates NF-kappa B without proteolytic degradation of I kappa B-alpha. Cell. 1996 Sep 6;86(5):787-98.

60. Yasunari Takada, Asok Mukhopadhyay, Gopal C Kundu, Ganapati H Mahabeleshwar, Sujay Singh, Bharat B Aggarwal. Hydrogen peroxide activates NF-kappa B through tyrosine phosphorylation of I kappa B alpha and serine phosphorylation of p65: evidence for the involvement of I kappa B alpha kinase and Syk protein-tyrosine kinase. The Journal of Biological Chemistry. 2003 Jun 27;278(26):24233-41.

61. Chun Chen, Zhuo-Qing Xu, Ya-Ping Zong, Bao-Chi Ou, Xiao-Hui Shen, Hao Feng, Min-Hua Zheng, Jing-Kun Zhao, Ai-Guo Lu. CXCL5 induces tumor angiogenesis via enhancing the expression of FOXD1 mediated by the AKT/NF-κB pathway in colorectal cancer. Cell Death & Disease. 2019 Feb 21;10(3):178.

62. Timothy Chao, Emma E Furth, Robert H Vonderheide. CXCR2-Dependent Accumulation of Tumor-Associated Neutrophils Regulates T-cell Immunity in Pancreatic Ductal Adenocarcinoma. Cancer Immunology Research. 2016 Nov;4(11):968-982.

ABSTRACT (IN KOREAN)

구강편평상피세포암 침습에서 CXCL5–CXCR2의 역할

<지도교수 정 원 윤>

연세대학교 대학원 응용생명과학과

김 형 근

구강편평상피세포암은 전세계적으로 구강에서 가장 흔한 악성 신생물이다. 해부학적으로, 구강편평상피세포암은 쉽게 상악골과 하악골로 침습하며, 뼈 침습이 진행된 환자는 예후가 좋지 않다. 본 연구에서는 구강편평상피세포암의 침습에서 CXCL5와 수용체 CXCR2의 역할 및 하위 신호전달을 통해 조절되는 표적 분자를 규명하였다.

먼저, 구강편평상피세포암의 침습에서 CXCL5와 CXCR2의 역할을 확인하였다. 구강편평상피세포암 세포에 CXCL5를 처리하였을 때 암세포의 침습이

촉진되었으며, CXCL5의 중화항체를 처리하였을 때는 침습이 억제되었다. 수용체인 CXCR2의 중화항체를 처리하거나 발현을 저하시켰을 때, 암세포의 침습이 억제되었으며, CXCL5에 의해 증가한 암세포의 침습도 현저히 억제되었다. 또한, CXCR2 발현이 억제된 구강편평상피세포암 세포는 침습능이 약한 조약돌 유사 형태를 보였다.

이어서, CXCL5를 처리한 구강편평상피세포암 세포에서 차세대염기서열분석법을 이용하여 전사체의 발현을 조사하였다. 전사체의 발현 변화를 기반으로 유전자 세트 증폭 분석을 수행한 결과, 인터페론 알파 반응 및 활성산소 신호전달 체계에 관련된 유전자 세트가 증폭되는 것을 확인하였다. 이들 유전자를 증폭시키는 전사활성을 규명하기 위해, 구강편평상피세포암 세포에 CXCL5를 처리하고 Cignal Finder 45-Pathway Reporter Array를 수행한 결과, NF-κB, HIF-1α, AP-1 전사인자의 활성이 촉진되었다. 구강편평상피세포암 세포에 CXCL5를 처리하고 웨스턴 블랏을 수행한 결과, NF-κB와 IκBα의 발현과 NF-κB, AKT의 인산화가 증가되었으며, CXCR2의 발현이 저하된 암세포에서는 CXCL5에 의한 NF-κB와 IκBα의 발현 및 NF-κB, AKT의 인산화 증가가 관찰되지 않았다. NF-κB 및 AKT 저해제와 CXCL5를 처리하였을 때, CXCL5에 의해 증가한 구강편평상피세포암의 침습이 유의적으로 억제되었다. NF-κB 저해제를 CXCL5와 같이 처리하였을 때, CXCL5에 의한 NF-κB, IκBα의 발현 증가가 나타나지 않았고 AKT의 활성화에는

영향을 미치지 않았다. AKT 저해제를 CXCL5와 같이 처리한 결과, CXCL5 처리에 의한 NF-κB와 IκBα의 발현과 AKT 인산화가 억제되었다.

생물정보학 분석을 통해 두경부암 조직에서 *CXCL5* mRNA 발현은 4단계 두경부암 조직에서 가장 높았으며, 환자의 좋지 않은 예후와 관련이 있었다. 또한, *CXCL5* mRNA 발현은 *NFKB1*과 *IKBA* mRNA 발현과 양성상관계를 보였다.

결론적으로, CXCL5는 CXCR2를 통해 AKT/NF-κB의 활성을 촉진하여 구강편평상피세포암 침습을 촉진한다. CXCL5, 수용체 CXCR2, 하위 표적 분자는 구강편평상피세포암의 침습을 예측하는데 유용한 생체표지자로 개발 가능성이 높다.

핵심 되는 말: 구강암, 구강편평상피세포암, 침습, CXCL5, CXCR2, NF-κB, AKT